[Scanning Electron Microscopy](https://digitalcommons.usu.edu/electron)

Volume 1985 | Number 3 Article 12

8-7-1985

The Cathodoluminescence Mode of the Scanning Electron Microscope: A Powerful Microcharacterization Technique

D. B. Holt
Imperial College of Science and Technology

F. M. Saba
Imperial College of Science and Technology

Follow this and additional works at: https://digitalcommons.usu.edu/electron

Part of the Biology Commons

Recommended Citation

Holt, D. B. and Saba, F. M. (1985) "The Cathodoluminescence Mode of the Scanning Electron Microscope: A Powerful Microcharacterization Technique," *Scanning Electron Microscopy*: Vol. 1985 : No. 3 , Article 12.
Available at: https://digitalcommons.usu.edu/electron/vol1985/iss3/12

This Article is brought to you for free and open access by the Western Dairy Center at DigitalCommons@USU. It has been accepted for inclusion in Scanning Electron Microscopy by an authorized administrator of DigitalCommons@USU. For more information, please contact digitalcommons@usu.edu.

SCANNING ELECTRON MICROSCOPY/1985/III (Pages 1023-1045)
SEM Inc., AMF O'Hare (Chicago), IL 60666-0507 USA

0586-5581/85$1.00+.05

THE CATHODOLUMINESCENCE MODE OF THE SCANNING ELECTRON MICROSCOPE: A POWERFUL MICROCHARACTERIZATION TECHNIQUE

D.B. Holt* and F.M. Saba

Department of Metallurgy & Materials Science, Imperial College of Science and Technology, London, SW7 2BP, U.K.

(Paper received March 01, 1984: manuscript received August 07, 1985)

Abstract

By detecting cathodoluminescence (CL) in a scanning electron microscope (SEM), pan and monochromatic micrographs and CL spectral analyses analogous to x-ray mode point analyses can be obtained. Complete microcharacterization requires alternate examination of both micrographs and spectra. New techniques for near infra-red CL and low-temperatures to produce sharp spectra are of increasing importance. CL emission is due to electron transitions between quantum mechanical states so the radiative defects present can be unambiguously identified at liquid helium temperatures. Strongly luminescent impurities can be detected to below one part in 10^8. This is 10^4 times as sensitive as the x-ray mode (electron probe microanalysis). Only luminescent impurities can be detected and quantitative analyses by CL have not yet been attempted. There is a rapidly increasing use of the CL mode for the study of industrially important problems and for the study of the electronic effects of dislocations in semiconductors.

Key Words: Cathodoluminescence, scanning electron microscopy, microcharacterization, semiconductors, photoluminescence analysis, low temperature, infra-red, recombination,microanalysis.

*Address for correspondence:
D.B. Holt
Department of Metallurgy & Materials Science
Imperial College of Science and Technology
London, SW7 2BP, U.K.
Phone no.: 01 589 5111 Ext. 6012

Introduction

The cathodoluminescence (CL) mode of scanning electron microscopy (SEM) is rapidly developing (Holt and Datta (1980), Holt (1981, (1985)). It is now recognized as an important technique not only for the characterization of optoelectronic materials and devices (Davidson and Dimitriadis (1980), Booker (1981), Lohnert and Kubalek (1983)) but also for applications ranging from ceramics through glass and polymers to biological and medical phenomena (Brocker and Pfefferkorn (1978, 1980), Pfefferkorn et al (1980), Holt (1984)).

Cathodoluminescence is the emission of light as the result of "cathode ray" i.e. electron bombardment. It is the mechanism whereby television (TV) pictures, cathode ray oscilloscope (CRO) traces, computer monitor displays and transmission electron microscopy (TEM) and scanning electron microscopy (SEM) micrographs on "fluorescent" screens are seen. Thus CL is an important technological phenomenon and the subject of much research and development. Photoluminescence (PL) is the emission of light as the result of photon (ultraviolet or laser) excitation. It is of industrial importance as it is the mechanism of emission in "fluorescent" lights. It is also a well-developed technique for the study of solids (Bebb and Williams (1972), Williams and Bebb (1972), Ashen et al (1975) and Dean (1982)). It is necessary to check that the subtle differences that are possible between PL and CL do not invalidate the comparison, but then the PL data can be used to identify CL emission mechanisms and interpret CL data.

Light, in and near the visible range, is emitted as the result of electron transitions between quantum mechanical states separated by about 1 to 3.5 eV. In solids, such states are separated by the whole, or a large part, of the forbidden energy gap between the filled valence band and the empty conduction band of semiconducting and insulating materials. In hydrocarbons, the transitions are between molecular orbitals that are described as triplet or singlet states. For simplicity, and because the phenomena of luminescence in wide gap solids have been more thoroughly studied we will confine our attention here to such materials. For further information on molecular cathodoluminescence see Pfefferkorn

et al (1980) and Holt (1984b) and the literature references in Brocker and Pfefferkorn (1978, 1980).

A useful distinction is that between intrinsic, fundamental or edge CL emission on the one hand and extrinsic, activated or characteristic CL on the other. The types of emission mechanisms involved in the two cases are illustrated in Figure 1.

CL which, at and near room temperature, appears as a band of wavelengths with its intensity peak at a photon energy:

$$h\nu_f = Eg \tag{1}$$

is produced by recombination of electrons and holes, generated by electron bombardment, across the forbidden energy gap. It arises from the "fundamental" energy band structure "intrinsic" to the material. It is produced by the inverse of the mechanism responsible for the absorption "edge" of the material, hence the alternative names by which this CL band is known. This account is adequate for the broad fundamental band seen at room temperature and down to liquid nitrogen temperatures, say. Any variable that affects the value of Eg can be determined by measuring $h\nu_f$. This has been used to determine local variations in temperature, high impurity doping concentrations and crystal structure in polymorphic materials. For reviews of this early work see e.g. Davidson (1977) and Holt and Datta (1980).

At liquid helium temperatures, the fundamental band resolves into line spectra as will be discussed below. An important distinction in this context is that between direct and indirect gap electron energy band materials as shown in Figure 2. Only in direct-gap materials is "direct" radiative band - band recombination of electrons and holes a significant process. Only in such materials is this fundamental CL emission observed. Edge emission at liquid helium temperatures has come to have a quite different meaning as we shall see below.

CL-emitting electron transitions that begin or end, or both, on localized energy states in the forbidden energy gap can only occur as a result of the presence of point defects giving rise to such states. These defects are known as luminescence centres or radiative recombination centres. They are "extrinsic" to the material. Such emission bands are "activated" by impurity atoms or other point defects and the emission is "characteristic" of the particular activator. Hence the descriptive names used for these varied CL emission bands. A wealth of information about luminescent point and other defects is obtainable and it is in this aspect that the CL mode has advanced most rapidly.

An introductory account of the CL mode will be given next followed by a review of some of the most significant recent advances.

Panchromatic and Monochromatic Microscopy

Figure 3 is a schematic diagram of a typical early detection system for visible CL. The output from the photomultiplier is the signal. It can be operated to produce micrographs or spectra.

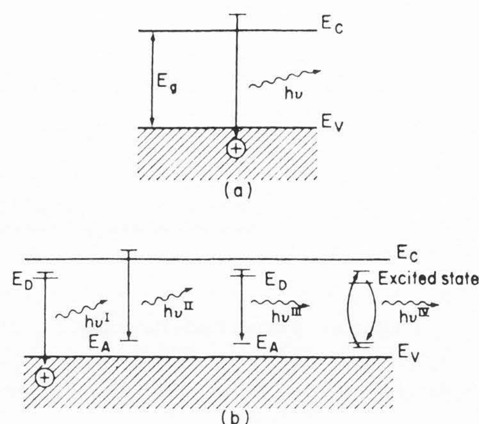

Fig. 1. Schematic diagram of the emission mechanisms producing (a) intrinsic and (b) extrinsic CL. The photons of energies I to III result from recombination of electrons and holes. The photon of energy IV is produced by radiative de-excitation of a centre such as a rare earth ion.

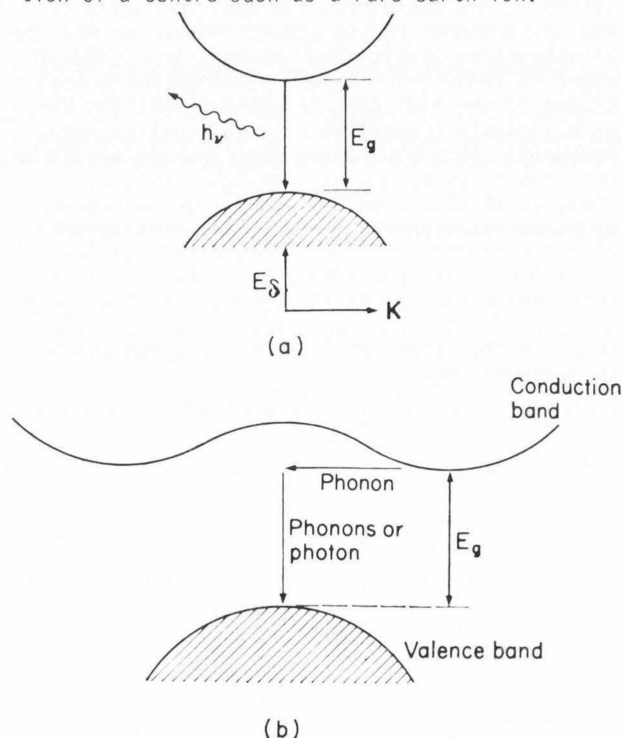

Fig. 2. Direct and indirect gap energy bands. (a) direct gap: vertical radiative transitions can take place between the conduction band minimum and the valence band maximum as they are at the same (Γ) point in k space so spontaneous band to band electron-hole recombination has a significant probability. (b) indirect gap: electrons in the conduction band minimum and holes at the valence band maximum differ in k and, hence, momentum so radiative recombination has a negligible probability.

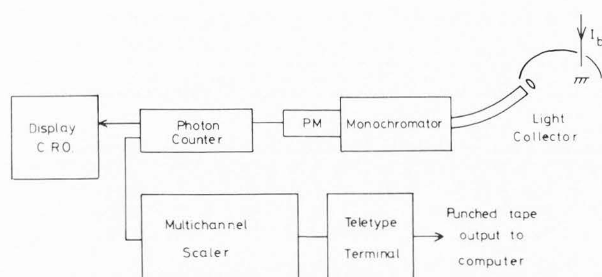

Fig. 3. Schematic diagram of a typical detection system used for visible CL.

For monochromatic micrographs the monochromator setting is constant and the beam is scanned over the specimen. For spectral "point analyses", the beam is stationary or scans a small selected area while the monochromator is stepped through the wavelength range of interest.

If the grating in the monochromator is bypassed e.g. by swinging a mirror in front of it, light of all wavelengths falls on the photomultiplier. This gives the panchromatic or integral CL signal. Used as video signal it produces panchromatic CL micrographs showing the more and less strongly luminescent regions in the specimen. This is all that can be done if the CL intensity is low relative to the sensitivity of the detector or if, as in the case of many organic materials, the specimen is rapidly damaged by electron bombardment. Panchromatic microscopy is used for optimising the operating conditions of the microscope and the detection system. It is also used to determine whether the particular specimen emits sufficiently strongly to be analysed and to find the brightest regions for spectral characterization. In industry it is often all that is needed for trouble shooting and quality assurance testing.

By setting the grating and the slits of the monochromator to transmit a particular wavelength range of interest, monochromatic CL micrographs can be produced. These show where the particular emission mechanism responsible for that wavelength is strongly operative.

Energy Dissipation and Spatial Resolution

The resolution attainable is limited in principle by three quantities in some combination. These are the diameter of the incident beam on the specimen surface, the range of penetration of the electrons into the solid and for some luminescence mechanisms (those involving charge carrier recombination) the minority carrier diffusion length or the ambipolar diffusion length. The energy of the incident electron beam is dissipated throughout some roughly spherical volume of diameter about equal to the range. Electrons and holes diffuse out from this volume while recombining. In practice the resolution is generally about equal to the electron range though it is affected by the luminescence efficiency of the specimen and the sensitivity of the detection system used. For a simple account of the principles involved see Davidson (1977) and Davidson and Dimitriadis (1980). A mathematical treatment was published by Spivak et al (1977).

CL Spectral Analyses

CL point analysis spectra can be recorded as described above. If the response characteristic of the detection system has been determined the observed photomultiplier count rate can be corrected to give the spectrum in number of photons emitted per unit time per wavelength or photon energy resolution interval (Steyn et al (1976)). Such "absolute" spectra are more meaningful than the commonly-published "arbitrary units" spectra in the luminescence literature. They are also reproducible. Many of the published "arbitrary units" or "relative intensity" spectra are irreproducible. This seems to be because photomultipliers etc. of widely varying behaviour were used but this was not corrected for. These remarks apply particularly to the broad-band spectra obtained at temperatures in the liquid nitrogen to room temperature range. For line spectra recorded over narrow wavelength ranges at liquid helium temperatures, it is less important.

Spectral Resolution The spectral resolution attainable is dependent on the characteristics of the detection system, the luminescence efficiency of the specimen and its temperature. In our experience, at liquid nitrogen to room temperature, with the detection systems of Figures 3 and 5, for even the brightest materials, resolution is specimen limited. That is, the system is operated with a large monochromator-slit width to maximise the photon count rate at the cost of resolution. At liquid helium temperatures, where emission lines are narrow and intense, the resolution attainable is monochromator limited.

Extrinsic and Intrinsic CL

In the CL spectra near room temperature the intrinsic and extrinsic emission bands are readily distinguishable. If the band gap energy, E_g , for the material is known, the intrinsic band can be identified using equation (1). The intrinsic band, if present, occurs at the highest photon energy $h\nu$, i.e., at the shortest wavelength, λ , emitted. If the gap is too large e.g., in diamond, the intrinsic band will fall in the ultra-violet, outside the detection limits of most detection systems.

Deep level extrinsic CL mechanisms will give rise to emission bands at lower photon energies i.e., at longer wavelengths than the intrinsic emission. Several situations can arise that make analysis of CL in any detail difficult or impossible. The two most frequently encountered e.g., in minerals, are long decay time emissions and numerous overlapping emission bands at higher temperatures.

The effect of long decay time CL on panchromatic micrographs is to produce smearing. That is, long streaks appear in the scan direction starting at the emitting point and continuing until the emission intensity falls below the detection limit of the system as shown in the case of mineralogical sphalerite (cubic ZnS) in Figure 4. The only solution to such a problem is to avoid areas giving such emissions

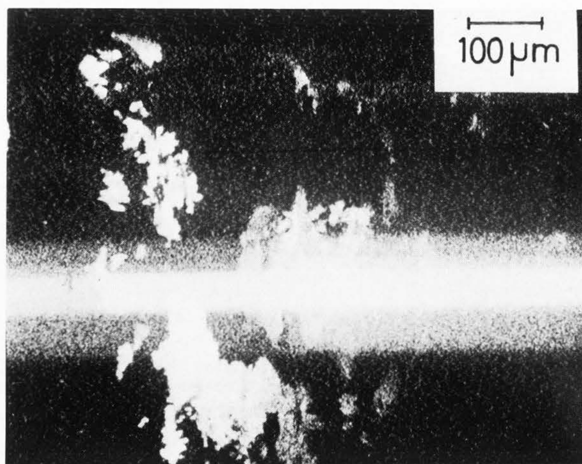

Fig. 4. Panchromatic CL micrograph of mineralogical ZnS showing smearing (the broad bright horizontal band) due to a grain emitting brightly with a long decay time after bombardment. (After Steyn et al, (1976)).

or to record only point analyses and monochromatic micrographs for wavelengths well away from the long-decay emission band. To overcome the problem of numerous overlapping bands there are two possibilities. By lowering the temperature, the bands may be narrowed so they no longer overlap. If the shape of the bands is known "band stripping routines" like those used in x-ray microanalysis could be applied. That is, the positions and intensities of the overlapping bands could be found by computation. At present no such information is available in general, however (Yacobi et al (1978, 1979).

Luminescence Microcharacterization

Alternating use of panchromatic microscopy, spectral point analyses and monochromatic microscopy makes it possible to disentangle the effects due to several causes operating in the same specimen. An example of this was the work of Datta et al (1977) on striated ZnS platelet crystals where the effects of changes of crystal structure, impurity segregation and of electrical fields at phase interfaces were identified and their locations found. Particular CL emission mechanisms can be identified in the CL spectra. Monochromatic micrographs using the appropriate wavelength show where that mechanism is operative e.g., where that impurity is concentrated.

Instrumental Developments

The intensity of CL emitted in the SEM is small. Maximum CL intensities over the whole spectrum range from microwatts downward, often by many orders of magnitude. Hence the most essential feature of CL detection system designs is the highest possible efficiency of light collection, transmission and detection. For light in the visible range, approximately 350 to 750 nm, photomultipliers are almost always used and many CL detection system designs for wavelength and/or lifetime resolution have been published. This literature was reviewed previously (Holt (1981)).

A computerized version of the conventional visible CL spectroscopic detection system of Figure 3 is shown in Figure 5. The addition of a computer-controlled stepper motor drive to the system makes signal averaging possible. That is the spectrum can be repeatedly recorded by stepping the monochromator up and down over the chosen wavelength range.

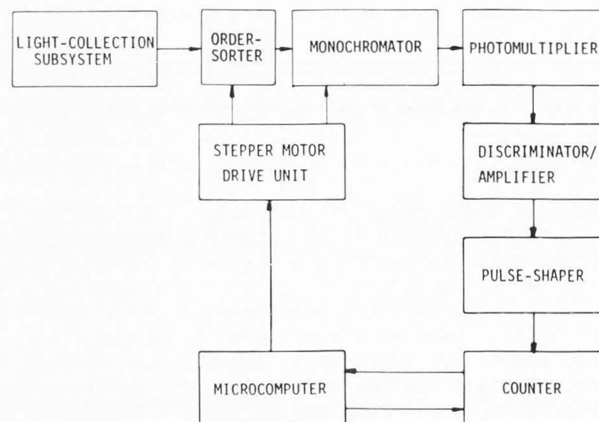

Fig. 5. A computerized CL detection system of the type shown in Figure 2. (After Saba and Holt (1983)).

Adding these data, the noise averages out, leaving the signal clearly visible as shown in Figure 6. The improvement in signal/noise ratio obtained is important for weak emission bands. In addition the data can be immediately corrected and printed out (Figure 6 contains uncorrected microcomputer graphics data to show the effect of signal averaging on the experimental observations). Feedback control programs can be used e.g., to step the monochromator slowly through spectral regions containing CL emission but fast where there is none. This saves time and minimizes possible beam damage and contamination build-up. Many CL detection systems are now computerized and this trend will continue.

Infra-Red CL

There is intense interest in materials with energy gaps corresponding to fundamental emission (equation (1)) at 1.3 and 1.55 µm for fibre optic communication systems. The energy gap of Si is about 1.1 eV which corresponds by a convenient coincidence to fundamental CL emission at about 1.1 µm at room temperature. All these wavelengths lie in the near infra-red so photomultipliers cannot be used, which is a severe handicap. Photomultipliers give output pulses of about a million electrons for each electron released from the photocathode and have gain-bandwidth products that are outstanding for any form of amplifier.

For infra-red detection photoconductive or photovoltaic semiconductor detectors have to be used. These give gains of unity to a few

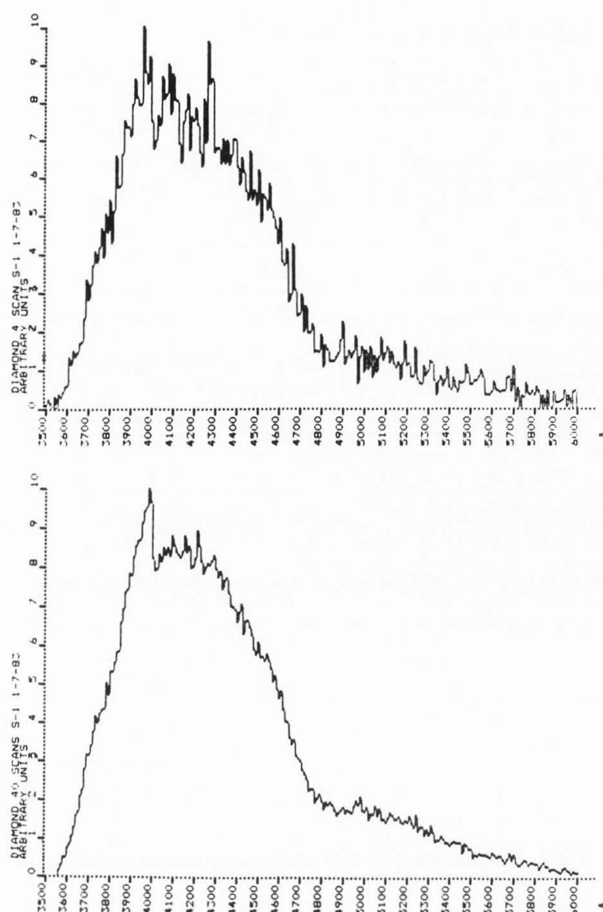

Fig. 6. The CL spectrum of a synthetic diamond recorded with signal averaging over four (upper figure) and forty (lower figure) recordings at room temperature. (F.M. Saba, unpublished results (1983)).

hundred. Hence it is best to abandon wavelength-dispersive monochromators as used for spectroscopy of visible CL. Monochromators with Ge detectors have been used with some success spectroscopically, however. For panchromatic microscopy Chin et al (1979) used a Si photodiode and Chin (1982) used both Ge and Si detectors. The detector can be placed below the specimen in which e.g. the substrate, of wider gap, is transparent to the infra-red from the top epitaxial layer. This was termed transmission CL (TCL) by Chin et al (1976). If the detector is placed above or to one side of the specimen (Chin (1982)) the technique may be called emitted CL (ECL) (Cocito et al (1983)). By employing both Ge and Si detectors, which have different wavelength sensitivities, in both positions, the technique can be made very effective for the analysis of e.g. double heterostructure materials (Cocito et al (1983)).

The optimum spectral analysis method in the infra-red is Fourier transform spectrometry with circular variable filters for monochromatic microscopy. Circular variable filters (CVFs) + are interference filters deposited on 180° sectors of circular substrates. The deposited film thickness, and therefore the center wavelength of the narrow passband, varies linearly with angular position round the substrate. Thus a near infrared CVF will pass a narrow band of wavelengths and this can be varied continuously by rotating the filter in the path of the light beam. The Fourier transform spectrometer (FTS) is generally based on the Michelson interferometer, as shown in Figure 7(a), which produces the interferogram of the infra-red CL emission as one mirror is moved. The interference pattern is transduced by a photodetector and converted into a suitable form for processing by a computer. Fast Fourier transform (FFT) methods, such as those based on the Cooley-Tukey algorithm are used to obtain the CL spectrum by computing the Fourier transform of this data (Cooley and Tukey (1965)).

The FTS has two main advantages over the monochromator: the multiplex or Fellgett's advantage and the throughput or Jacquinot's advantage. The former refers to the signal/noise gain provided by the FTS when the noise is independent of the signal level, as in the case when semiconductor photodetectors are used. This gain results from the FTS responding to all the spectral elements of the input signal simultaneously (hence "multiplex"), as opposed to each element being recorded sequentially by the monochromator. For a total detection time T and N spectral elements, the monochromator therefore spends only a time T/N for each element, which leads to a gain of the order of $\sqrt{N}$ for the FTS.

The greater optical throughput possible with the Michelson interferometer, because it does not need entry and exit slits, leads to the Jacquinot's throughput advantage. This gain gives the FTS a superior performance even when Fellgett's advantage disappears due to the noise varying as the square root of the signal level, as in the case when photomultipliers are used for observing visible and ultra-violet emissions. (For more detailed accounts of Fourier transform spectroscopy see Horlick (1968), Schopper and Thompson (1974) and Sakai (1977)).

The resolution of the FTS depends mainly on the maximum optical path difference L between the two arms of the interferometer and is given by:

$$\delta\sigma = 1/2L \qquad (2)$$

This shows that a high-resolution instrument for the near infra-red can be quite compact. The largest sampling distance d which can be used before different orders overlap is:

$$d = 1/2\sigma_M \qquad (3)$$

+ available from OCLI, Box 1599, Santa Rosa, California 95402, U.S.A.

where σ_M is the reciprocal of the shortest wavelength detected. The number of independent data points N is then given by:

$$N = L/d = 2L\sigma_M \quad (4)$$

and the resolving power is:

$$R = \sigma_M/\delta\sigma = N/2L = N \quad (5)$$

which means that the resolving power depends on the number of independent data points. This number is mainly limited by the distance the moving mirror can travel and the processing time required for computing the Fourier transform.

Panchromatic signals could be obtained by holding the moving mirror at the point of zero path difference. Monochromatic microscopy would then be a simple matter of inserting a suitable filter in the input beam.

By using an infra-red sensitive semiconductor (e.g., Ge) detector and a suitable grating, monochromator detection systems can also be used and Figure 7(b) shows such a system used successfully on a TEM and an example of a spectrum recorded by this system is shown in Figure 11. A direct comparison of the same spectrum recorded using a monochromator and an FTS in Figure 8 demonstrates the advantage of the latter with respect to noise.

CL Decay Rate Measurements

Let the intensity of a particular CL emission band under continuous bombardment be L(0). If the beam is chopped at a time t = 0, a decay time τ_d can be obtained in those cases in which the decay has the simple exponential form:

$$L(t) = L(0)\exp(-t/\tau_d) \quad (6)$$

Beam-chopping lifetime measurements had been developed early for use in charge collection (electron beam induced current - EBIC) measurements. They were extended to "time-resolved CL" studies by Balk et al (1975) using a photomultiplier followed by a boxcar integrator and a recorder and by Rasul and Davidson (1977) who used the photon counting method to follow the decay of the emission rate. In these techniques the decay of each emission band has to be measured separately, "sequentially" (Pfefferkorn et al (1980)). Hastenrath et al (1977) simultaneously registered the decays of all the emission bands using as the detection system a streak camera observed by a silicon intensified target (SIT) electronic camera. The output of this was fed into an optical multi-channel analyser (OMA). The streak camera can determine decay times from 10 ns to 300 ns so this system is suited to measuring fast decay phenomena.

CL on Dedicated STEM Instruments

Pennycook et al (1980) developed a CL collection system usable in the restricted specimen space and ultra-high vacuum environment of a field-emission gun Crewe scanning transmission electron microscope (STEM) and Petroff et al (1980) also have a CL detection

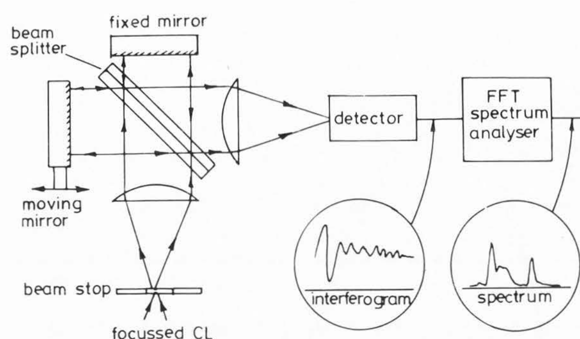

Fig. 7. Schematic diagrams of two types of infrared CL detection systems: (a) a Fourier transform spectrometer (after Davidson et al (1981)) and

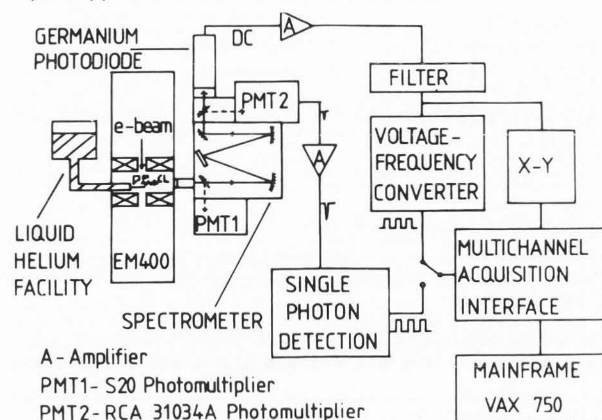

(b) a wavelength dispersive monochromator system (After Myhajlenko (1984).

system on such an instrument. These microscopes make possible STEM, CL and EBIC observations on the same defects as shown in Figure 18. Such observations are more directly intercomparable than for example EBIC and TEM micrographs recorded on different instruments, sometimes with thinning carried out between the observations. Thus far the thinness of the specimens and the very small CL intensities emitted have made the STEM CL technique difficult.

Low Temperature CL

In earlier reviews (Holt and Datta (1980), Holt (1981)) the importance of reducing specimens to liquid helium temperatures was emphasised and the design of a stage for such work, based on a commercial Oxford Instruments continuous flow cryostat system was reported. The use of liquid helium temperatures is doubly beneficial. Many CL emission bands become much more intense as well as much sharper as thermal broadening is reduced. CL band emission rates often increase by factors of five to ten and the intensity of the red emission from quartz increases by three orders of magnitude (P.R. Grant, private communication) from room temperature to liquid helium temperatures. This can improve the signal to noise ratio sufficiently to make microscopy possible,

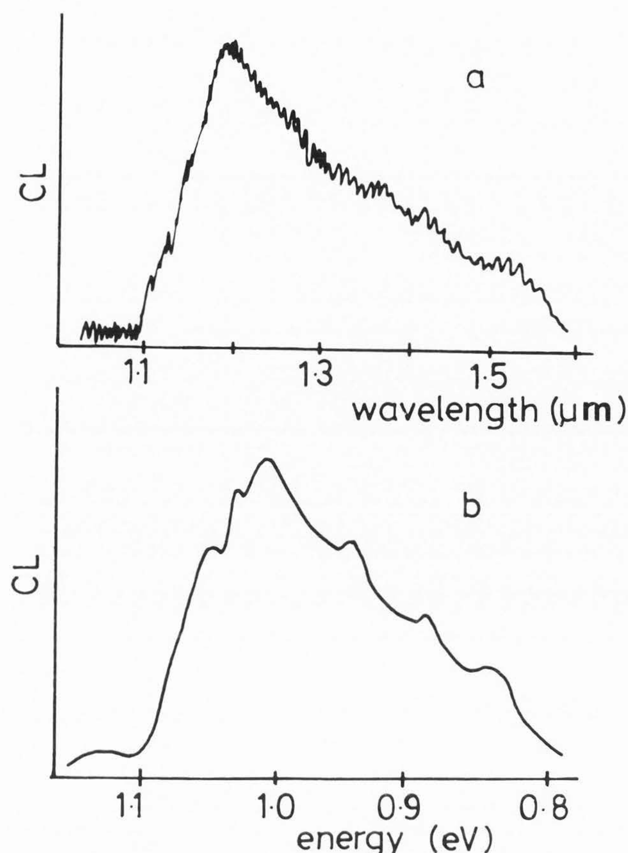

Fig. 8. A comparison of spectra from Cr-doped GaP recorded using (a) a grating spectrometer and (b) a Fourier transform spectrometer (After Davidson et al (1981)).

as the example in Holt (1981) demonstrated. Damage in organic materials is slowed (Hörl and Roschger (1980)) and the use of computerized frame storage and image processing of micrographs should extend the CL technique more widely into the medical and biological fields. In addition, the sharp emission line series observable at liquid helium temperatures can be interpreted in fundamental terms for the unambiguous identification of luminescence centres. A number of liquid helium stages for the CL mode are known to be in use and the Oxford Instruments model is available commercially+. Hence there is a rapid increase in the use of the technique for the identification of luminescent impurities and other point defects as will be reported below.

The extrinsic emission mechanisms are more varied as indicated in Figure 1(b) than in the case of intrinsic CL (Figure 1(a)). However the luminescence centres involved can usefully be classified as (a) shallow and deep recombination centres and (b) excitation/de-excitation centres. Shallow and deep are terms used in the semiconductor literature to distinguish between states such as E_D and E_A in Figure 1(b) which are less than (shallow) or more than kT from the adjacent band edge (deep). Excitation and de-excitation are terms used in the luminescence literature. They describe the processes of raising a centre like that at the right in Figure 1(b) from its ground state and then radiatively dropping it back to that ground state. Such transitions are internal to the centre and do not involve electrons in Bloch function states belonging to the crystal.

The classical shallow level impurities are the donors and acceptors in Si. The binding of the electrons in these cases is so weak and the wave functions fill so large a volume that the well-known effective mass approximation can be applied. At the opposite extreme of tight binding, as exemplified by the radiative (de-excitation) transitions in rare earth ions such as Eu^{+3}, atomic wave functions can be successfully used. Most impurities fall into the intermediate category in which both the crystal potential and the local atomic potential are significant. The Greens function approach is proving most useful for such cases since the Hamiltonian can then be written in terms of the sum of the periodic (crystal) potential and the atomic potential (Bernholc et al (1981)).

Radiative Recombination and Radiative De-Excitation

This distinction is not sharp but it is useful. Radiative recombination mechanisms are those that compete with other electron-hole recombination mechanisms, both radiative and non-radiative. The three basic cases are shown in Figure 1(b). A well-known mechanism is that of the recombination of an electron trapped on a donor with a hole trapped on an acceptor (mechanism III in Figure 1(b)). This is known as the donor acceptor pair (DAP) mechanism and will be treated below. The important practical example of DAP emission is that of O-Zn emission from GaP red light emitting diodes (LEDs). Radiative and non-radiative recombination mechanisms were reviewed by Mott (1978).

Radiative de-excitation mechanisms involve centres that are raised to excited electronic states by inelastic collisions with incident beam electrons or by indirect energy transfer mechanisms, and relax back internally to the ground state by emitting a photon. Such centres can often be treated by means of the well-known configuration coordinate model (Holt and Datta (1980)). They do not generally act as competitive recombination "channels" for electron-hole pairs. In the best known examples of such centres, like the rare earth ions in oxides, the emissive transition occurs between states only slightly modified from atomic levels.

Modified Ionic De-excitation Emission from Rare Earths and Transition Metals

The emissions from rare earth ions are due to transitions of shielded, inner d or f shell electrons. These inner shells have diameters that are only about half the ionic diameters so their shielding from the crystal potential by

+ from Oxford Instruments Ltd., Osney Mead, Oxford OX2 ODX, UK.

the outer s and p shell electrons, is very effective. The ground and excited state energies are virtually those of the free ions. The emission mechanism in a number of transition metals is similar, but the shielding is less effective and the crystal has a greater perturbing effect. Important examples of these types are the Cr (transition metal) ions responsible for ruby laser emission, and the Eu (rare earth) ions responsible for the red light from TV screens and some "fluorescent" phosphors. (Blasse (1978)). The Eu ion emission is independent of the host crystal only within certain limits. It makes a considerable difference whether the ion is doubly or triply positively charged. It is also important whether the site occupied has centrosymmetry or not. An account of these matters was written by Blasse (1978).

Recombination Centres: Recombination Times and Emission Rates

Competition occurs in the energy-dissipation plus diffusion volume, between the various radiative and non-radiative centres, for the recombination of the hole-electron pairs. To such processes the standard semiconductor recombination statistics apply. The radiative recombination efficiency of the ith type of centre i.e., the fraction of hole-electron pairs that recombine and emit photons in the ith band, is given by the ratio of the rate of radiative recombination R_{rri} to the total recombination rate R.

$$\eta_{rri} = R_{rri}/R = \tau/\tau_{rri} \qquad (7)$$

where τ_{rri} is the recombination time for the ith radiative centres and τ is the observable minority carrier lifetime, since the recombination rates are inversely proportional to the recombination times. The minority carrier lifetime is determined by the various recombination times as:

$$1/\tau = 1/\tau_{rri} + 1/\tau_{nri} \qquad (8)$$

where τ_{nri} is the effective recombination time due to all the other recombination channels. In fact it is made up of the remaining radiative (τ_{rr}) and non-radiative (τ_{nr}) recombination times as follows:

$$\frac{1}{\tau_{nri}} = \sum_j \frac{1}{\tau_{rrj}} + \sum_j \frac{1}{\tau_{nrj}} \qquad (9)$$

The other radiative recombination centres are lumped into τ_{nri} because they do not contribute to radiation in the ith CL band. Thus the rate of CL emission in the ith band, which is proportional to the efficiency η_{rri} can be written as:

$$L_i \propto R_{rri}/(R_{rri} + R_{nri}) = 1/\tau_{rri}/(1/\tau_{rri} + \tau_{nri}) = \tau_{nri}/(\tau_{rri} + \tau_{nri}) \qquad (10)$$

Recent Applications of the CL Mode to Semiconductors

The volume of work published recently is so great that attention will have to be concentrated on a few fields of particular interest. These are liquid-helium temperature spectral analyses, studies of dislocation contrast and industrial trouble-shooting studies.

Low-Temperature CL Spectra and Emission Mechanisms

In liquid-helium temperature CL spectra from sufficiently pure and perfect materials a number of lines become resolved at photon energies near the band gap and the distinction between intrinsic and extrinsic emission of Figure 1 is not so significant. Direct and indirect electronic energy band structures are shown in Figure 2. Only in direct gap materials is radiative recombination of conduction band electrons with valence band holes i.e., band-band CL significant at low temperatures. Also, as is well-known, only direct gap materials exhibit injection laser action i.e., stimulated emission of recombination radiation. The range of possible near band gap luminescence recombination mechanisms in a direct gap material like GaAs is shown schematically in Figure 9.

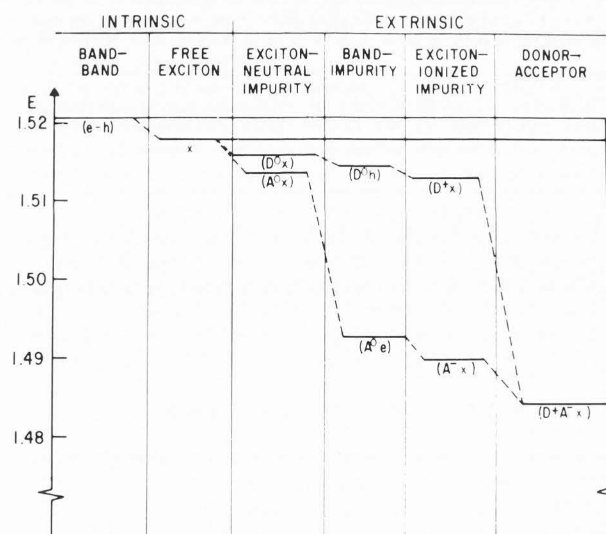

Fig. 9. Possible no-phonon emission lines for a direct gap III-V material such as GaAs at liquid helium temperatures. e and h are electrons and holes, x is an exciton, D and A are donors and acceptors and the superscripts are the charge states of these impurities. Thus A^- x is emission by recombination of an exciton bound to a negatively charged acceptor. The possibility of impurity interactions has been neglected. (After Bebb and Williams (1972)). The quantitative values are superseded by the later data of Table 1.

Table 1. The Photon Energies of Extrinsic (Free to Bound) Emission Peaks and the Energy Depths of Impurity Levels in Gallium Arsenide at 4.2 K.

Donors

$h\nu$ in eV	E_d in meV	References
Si 1.514	5-6	Almassy et al., 1981
S "	"	"
Se "	"	"
Te "	"	"
Sn "	"	"

Acceptors

$h\nu$ in eV	E_A in meV	References
C 1.494	26	Ashen et al., 1975
Si 1.485	35	"
Ge 1.479	41	"
Zn 1.489	31	"
Be 1.492	28	"
Mg 1.491	29	"
Cd 1.485	34	

Deep Level Impurities

$h\nu$ in eV	E_c in meV	References
Cu 1.306	160	Queisser & Fuller, 1966
Mn 1.407	113	Yu & Park, 1979
Sn 1.349	171	Ashen et al., 1975

TABLE 2

Observed lines in cathodoluminescence spectrum

Line	Energy (eV)	Assignment
	1.376	D-A pair (Zn)
A	1.359	D_oX
B	1.350	D_oX - TA
C	1.340	D_oX - LA
	1.331	D-A pair - LO
D	1.322	D_oX - TO
E	1.317	D_oX - LO
		D_oX - Loc
F	1.308	D_oX - TA - Loc
G	1.299	D_oX - LA - Loc
	1.290	D-A pair - Loc
H	1.282	D_oX - TO - Loc
I	1.276	D_oX - LO - Loc
		D_oX - 2Loc
J	1.268	D_oX - TA - 2Loc
K	1.259	D_oX - LA - 2Loc

Phonon designation:- TA = Transverse Acoustic
LA = Longitudinal Acoustic
TO = Transverse Optic
LO = Longitudinal Optic
Loc = Local Mode

The other symbols are as in Figure 9.

The Band-Band and Edge Emission Mechanisms

Edge emission at liquid helium temperatures has come to mean something quite different from band-band emission (Figure 9) which is the simple (Figure 1(a)) picture of fundamental or edge band emission at higher temperatures. A series of emission lines seen at low temperatures at approximately the band gap energy in II-VI compounds were termed the "edge emission". These were accounted for by Hopfield (1959) using a trapping model and an interaction Hamilton in which a carrier interacts with LO (longitudinal optical) modes of lattice vibration. This accounts for the observed emission line due to radiative recombination via a shallow level with a photon energy of:

$$h\nu = E_g - E_c \qquad (11)$$

where E_c is the energy depth (from the nearest band edge) of the trap level of the centre. Further reductions in photon emission energies in Figure 9 are due to the increasing energy depths of the levels of charged acceptors and donors as compared to the uncharged impurities. In addition the model gives lines, called phonon replicas, of energies

$$h\nu = E_g - E_c - n\hbar w \qquad (12)$$

where $\hbar w$ is the energy of an LO phonon (quantum of lattice vibrational energy). These arise due to the emission of the energy $E_g - E_C$ partly as a photon and partly as n phonons. The theory

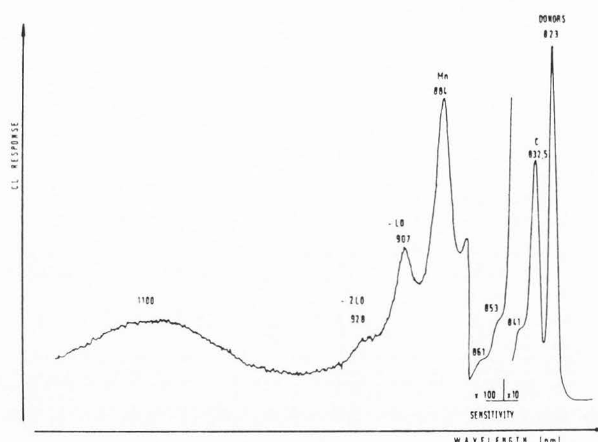

Fig. 10. Liquid helium (4.2 K) CL spectrum of accidentally contaminated MBE GaAs. There are clearly resolved narrow emission bands due to C and Ge and the contaminating Mn with two LO phonon replicas. (Wakefield, unpublished data.)

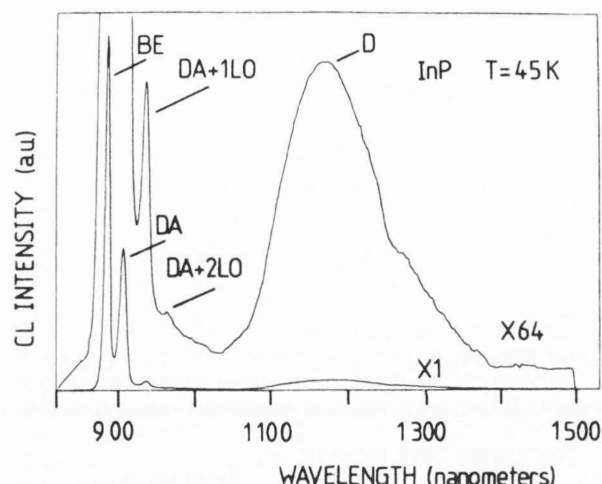

Fig. 11. CL spectrum of heat-treated InP at 35 K. The phonon replicas of the donor acceptor pair line are marked DA + LO and DA + 2LO. (After Myhajlenko (1984)).

led to a Poisson distribution of line intensities (photon emission rates) given by the probability of emission of n phonons with the photon:

$$W_n \simeq \tilde{N}^n / n! \qquad (13)$$

where $\tilde{N}$ is the mean number of LO phonons emitted. This gave good agreement with the observed energy separations and relative intensities of the lines in such materials as CdS, ZnS and ZnO. This was termed edge emission because E_C was small. Subsequently, a trap emission line and a set of LO phonon replicas, with the Poisson distribution of intensities of equation (13), was found in GaAs (Lee and Anderson (1964). The impurity involved (Mn) had a relatively deep level (large value of E_c) so $h\nu$ was well below E_g but the name edge emission was given to this phenomenon too. Figure 10 is a CL spectrum showing the first and second LO replicas of this distinctive series of Mn "edge" emission lines.

Donor, Acceptor and Donor-Acceptor Pair Recombination

Recombination via donor or acceptor states is illustrated in cases I and II in Figure 1(b). The energies of the photons emitted are given by equation (11) with E_D or E_A respectively substituted for E_C. In the case of donor-acceptor pair recombination shown as case III in Figure 1(b) the photon energy is given by:

$$h\nu = E_g - E_A - E_D + e^2/\varepsilon r \qquad (14)$$

where e is the charge on an electron, ε is the dielectric constant and r is the separation of the donor and acceptor sites in the crystal. The final term is too small to allow resolution of the lines corresponding to the possible small discrete values of r in the SEM at present. Instead the unresolved donor acceptor (DA) peak, arising from the many pairs with large values of r, so the final term is negligible, is seen. Examples of DA peaks or their phonon replicas are shown in the spectra of Figs. 11 and 12. In InP DA lines shift in energy and change to free-bound lines over the range from about 1 to 15 K.

Phonon Replicas

The phonon coupling of luminescence centres at higher temperatures is often discussed in terms of vibrational and electronic i.e. "vibronic" centre represented by a configuration coordinate diagram (Holt and Datta (1980)). An account of the configuration coordinate model in both classical and quantum mechanical terms will be found in Di Bartolo (1978). At low temperatures quantum mechanical methods like that of Hopfield (1959) for edge emission must be employed. Usually LO phonons are those appearing in low temperature spectra but phonons of all branches of the dispersion spectrum: LO and LA (longitudinal acoustic), TO (transverse optical) and TA (transverse acoustic), may play a role as well as phonons of local vibrational modes of the centre. Figure 12 is a CL spectrum containing many replicas corresponding to the emission of different types of phonon with the photon as identified in Table 2.

Exciton Recombination

At liquid nitrogen to liquid helium temperatures, in highly pure and perfect crystals an exciton line or lines may be resolved from the lower energy side of the fundamental band. Such lines have energies

$$h\nu_x = E_g - E_{x(n)} \qquad (15)$$

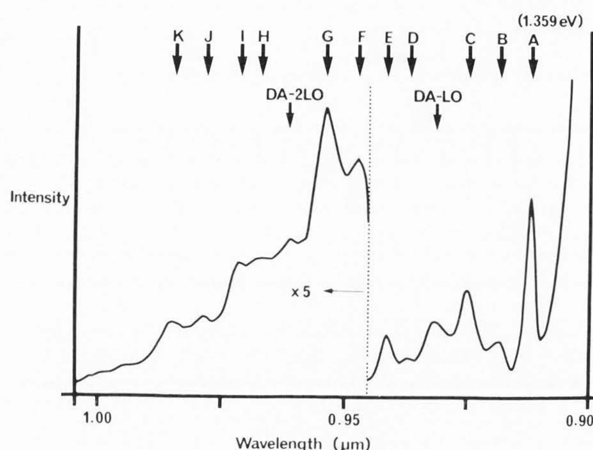

Fig. 12. CL spectrum of InP at liquid helium temperature showing a series of phonon replicas of a line at 1.359 eV, thought to be associated with a P vacancy. For the identification of the emission lines see Table 2. (Wakefield et al (1984a)).

where $E_{x(n)}$ is the binding energy of the nth state of an exciton i.e. of a coulombically bound hole-electron pair. Usually only the line corresponding to the ground state of the exciton is observed. Excitons that are free and those that are bound to impurities in various charge states can be distinguished by the photon energies emitted on recombination as shown in Figure 9 for GaAs. In Figure 11 BE is a bound exciton line.

Qualitative CL Microanalysis

Detailed fundamental studies of the low-temperature emission line spectra of many luminescence centres of both the recombination and excitation/de-excitation types have been published (see the bibliography in Holt and Datta (1980) and Bebb and Williams (1972), Williams and Bebb (1972), Ashen et al (1975) and Dean (1982)). By comparing observed spectra with such published data unambiguous identification of the emitting centres can often be made in a manner analogous to the identification of chemical elements by their characteristic X-ray emission line spectra in electron probe microanalysis.

As an example, Table 1 lists values of the energy depths of many important donors, acceptors and deep level impurities occurring in GaAs, which can be used for qualitative impurity identification in CL spectra by substitution into equation (11) or (14). In GaAs the acceptors are sufficiently well separated in energy to be identified but the donors cannot be at present.

The Detection Limit for the CL Method

The sensitivity of CL point analyses is demonstrated by the Mn peak in Figure 10. The concentration of Mn in this sample was found by SIMS (secondary ion mass spectrometry) working near its limit of detection to be 10^{14} atoms cm^{-3} or less. That is about one atom in 10^8 or 0.01 parts per million. This was readily resolved in Figure 10 despite the presence of an order of magnitude higher concentration of C and Ge. At best electron probe microanalysis (EPMA) can determine down to one part in 10^4. The demonstrated detection limit for the CL mode is thus 10^4 times better than that of the x-ray mode. The spatial resolutions of the two techniques are similar.

It can be argued (J.W. Steeds, private communication, 1983) that the detection limit for CL should be the same as that for PL since the advantages of these techniques should roughly balance. Dean (1982) concluded in a major review of the PL technique for semiconductor characterization that in the most favourable cases it should be possible to detect impurities down to 10^{12} atoms cm^{-3} which is 10^6 times better than for EPMA. The most favourable cases for CL microanalysis are those of impurities that are strongly luminescent and are present in host materials that do not emit or absorb significantly themselves nor contain other impurities that do so at the wavelength emitted by the impurity to be detected.

The drawbacks of the CL microcharacterization technique are that only luminescent impurities can be detected (but the x-ray and indeed all analytical techniques are also better for some elements than for others) and that as yet no attempts to quantify CL analyses have been made. This will be difficult, but not impossible. Now that the power of the technique has been so clearly demonstrated, it can be expected that work on the calculation of impurity or vacancy concentrations (see below) from CL data will begin.

Qualitative Microcharacterization by Low Temperature CL

A number of important practical applications of this technique have appeared in the three or four years that it has been in use. These have concerned applications to GaAs and InP.

Impurities in GaAs

In monitoring Molecular Beam Epitaxy GaAs one MBE system was found to produce p-type material although no dopant was added. The identification of Mn in the layers (Figure 10) led to the location of the source of contamination in a stainless steel component and a simple modification eliminated the problem.

Figure 13 shows the distribution of the main impurities found in undoped LEC (liquid encapsulated Czochralsaki) semi-insulating GaAs (Wakefield et al (1984b). This material has a structure of low dislocation density cells surrounded by dislocation tangles (Clark and Stirland (1981), Kamejima et al (1982), Stirland et al (1983)). The two luminescent centres detected in this material emit at 1.494 eV and 1.514 eV. The relative intensities of the two lines and the absolute intensities of the 1.494 line were found to vary between the cells and the

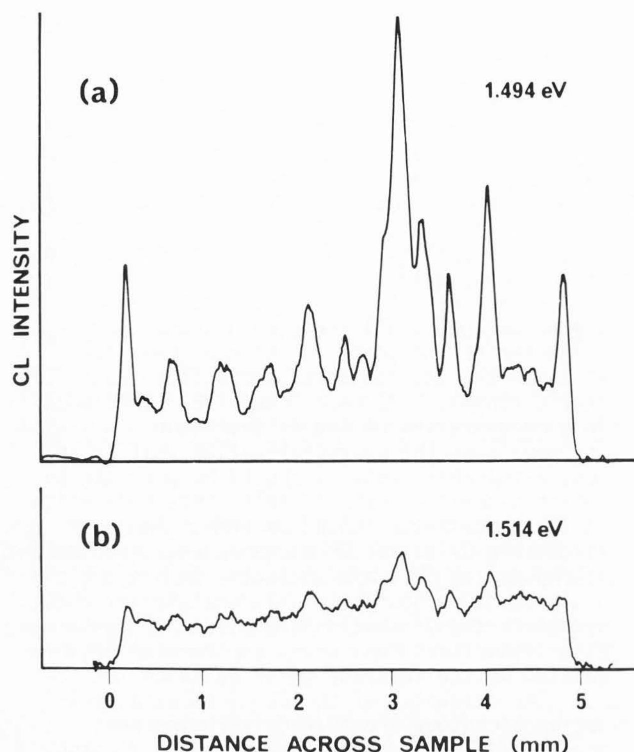

Fig. 13. Line scans of the intensity of CL at the photon energies of (a) 1.494 eV due to residual C and of (b) 1.514 eV associated with shallow donors or bound excitons, across an undoped LEC semi-insulating GaAs slice. (After Wakefield et al (1984b)).

dislocation tangles. The 1.494 eV line is due to carbon and the evidence of Figure 13 and of monochromatic CL micrographs was clearly that the carbon tended to segregate to the dislocation walls. It is likely that the carbon influences the conductivity and any resultant non-uniform conductivity would be serious for many applications.

Kamejima et al (1982) recorded both panchromatic CL linescans and SIMS linescans for Si, O and Cr impurities across semi-insulating GaAs slices. CL intensity maxima around the dislocation tangles correlated with impurity concentration peaks. The brighter regions around the tangles were ascribed to impurity depletion zones due to segregation to the dislocation lines. Dark contrast was seen due both to slip dislocations and some grown-in dislocations in the cell walls. Evidence of a variation of electrical properties between the cell interiors and walls was obtained by mechanical probing.

Impurities and Phophorus Vacancies in InP

Figure 11 is a spectrum from a sample of LEC InP annealed for 15 minutes at 750°C. There is a near band edge line due to excitons bound to shallow impurities marked BE and a donor-acceptor pair line DA with LO phonon replicas. In addition a deep level band marked D appeared which is ascribed to a phosphorus vacancy complex (Myhajlenko (1984)).

Figure 12 is a spectrum of InP containing a line at 1.359 eV together with many phonon replicas as identified in Table 2. This spectrum was found in MBE (molecular beam epitaxy) and MOCVD (metal-organic chemical vapour deposition) material grown under conditions likely to give rise to phosphorus deficiency (Wakefield et al (1984a)). Duncan et al (1984) reported a closely corresponding PL spectral line series in bulk n-type LEC InP which had been heated in vacuum at 900°C for 6 hours. Duncan et al showed that the line at 1.36 eV is due to the recombination of an exciton bound to a deep neutral donor i.e. to a D_o x process (Figure 9 and Table 2). The emission has been found only in P-deficient InP and it was suggested therefore that the defect responsible for the 1.36 eV emission is related to a complex involving a P vacancy. The ability of CL and PL to detect native point defects and/or complexes involving such defects is an additional attraction of the technique when compared to EPMA. Figure 12 also contains LO phonon replicas of a donor-acceptor pair emission. Deeper level emission bonds were studied by Temkin et al (1982) using PL. Some of these too were suggested to involve complexes including phosphorus vacancies.

SEM CL evidence of the non-uniform distribution of Ge in LEC InP was reported by Warwick and Booker (1983).

Applications of CL Methods to Practical Optoelectronics Problems

The use of CL as a tool for solving practical problems sometimes requires the most sophisticated detection systems and interpretive theories as in Figures 10 and 13. Much can often be accomplished without such refinements however.

Rogue Particles in Phosphor Powders

Richards et al (1984) showed SEM CL to be very useful for the study of "fluorescent" lighting phosphors which are powders of high photoluminescent efficiency. The inner surfaces of fluorescent tubes are coated with these materials. A gaseous discharge down the tube produces ultraviolet light which is absorbed in the phosphor and re-emitted at a longer wavelength in the visible. This is an example of a large Stokes shift (see e.g. Holt and Datta (1980)). The older fluorescent-light phosphors are complex "halophosphates" emitting a broad "white" band. These materials are intermediate pyrophosphates made in three stages. More recent phosphors are mixtures of narrower band emitters. These phosphors are known charmingly as CAT, BAM and YOE for Cerium magnesium Aluminate activated with Terbium, Barium Aluminate activated with Manganese and Yttrium Oxide activated with Europium, respectively. They emit in the green, blue and red. By varying the proportions of CAT, BAM and YOE a warmer (redder) light as preferred in the British market or a colder (bluer) light as preferred in continental European markets can be produced. The newer phosphor coatings on

fluorescent lights are thus complex powder mixtures in binders.

Traditional methods of analysis took months when applied to fluorescent coatings that do not have the efficiency or colour required. SEM CL can solve these problems in days because the combination of spatial and spectral analysis makes it possible to check the performance of the individual powder particles (Richards et al (1984)). Fortunately the CL and PL ("fluorescence") spectra of these phosphors are essentially the same. The CL properties of particular particles can thus be tested against the desired PL emission spectra. For example, in certain inadequately bright halophosphate phosphor coatings "rogue" particles were found. These gave CL spectra showing that the necessary Mn was absent. X-ray analysis showed that the Ca/K ratio was also too low. This sufficed to identify, within minutes, which one of the three heat treatments involved in making the phosphor had gone wrong.

An acceptable CAT particle should give three room temperature emission bands at 490, 550 and 590 nm. Bad CATs give broadened spectra as shown in Figure 14. The SEM micrographs in Figure 15 show that the non-uniformity in CL properties corresponds to the variation in the distribution of Al and Tr (terbium). Again this immediately identified the processing step that caused the anomalous emission.

This industrial application of CL has become a routine tool, with a purpose built CL instrument, based on an old EPMA machine, dedicated to the work (BP Richards, private communication). The production workers value it so highly that they are pressing for hot stage facilities for accelerated life testing to identify deterioration mechanisms.

CL Assessment of III-V Devices and Materials

The observation of dislocations in CL micrographs of GaAs (Schiller and Bois (1974)) [by the dot-and-halo contrast due to dopant segregation (see e.g. Holt (1974))] and of GaP (Werkhoven et al (1978/79)) have been widely used for materials assessment in industrial laboratories. The comparison of line scan traces of panchromatic CL and of CC (charge collection - usually EBIC - electron beam induced current) across GaP p-n junctions was early developed as a means of characterizing light emitting diodes (LEDs) (see e.g., Holt (1974)). Recent extensions and applications of this approach are the work of Acuna Rojas et al (1980), Haefner et al (1981) and Oelgart et al (1982). CL spectral studies of degradation in green emitting GaP LEDs were reported by Loehnert and Kubalek (1983) and Stegmann et al (1982). Stegmann et al (1982) also studied the temperature dependence of the CL in GaAsP doped with N. A CL study of degraded GaAlAs/GaAs double heterostructure lasers was published by Wakefield (1983). Transmission infrared CL (TCL) was used by Chin et al (1979) to evaluate the defects in InGaAsP epi-layers on InP. Dislocations threading through such layers are known to nucleate rapid degradation in GaAlAs - GaAs double heterostructure (DH) lasers (Petroff and Hartman (1973)) but not, apparently, in InGaAsP DH lasers.

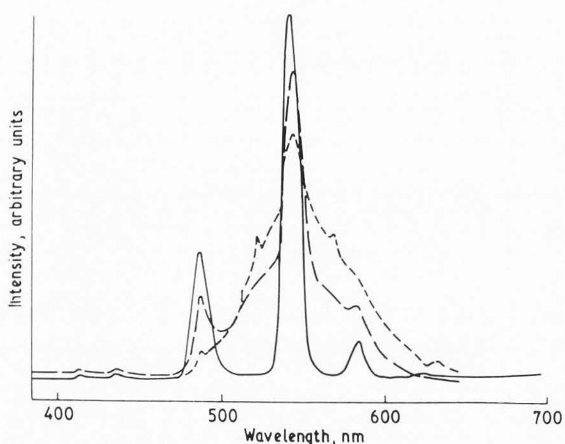

Fig. 14. CL spectra (continuous curve) from normal (white) and (dashed and dotted curves) anomalous (yellow) CAT phosphor particles. (After Richards et al (1984)).

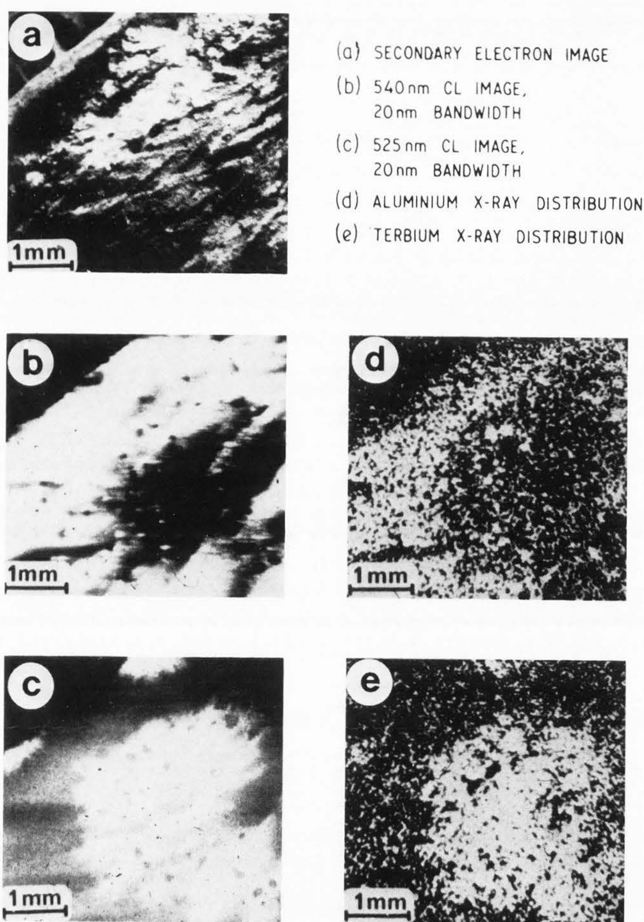

Fig. 15. SEM micrographs of a region of a CAT phosphor showing the surface appearance, the non-uniform emission of CL at 540 and 525 nm and the distribution of Al and Tr in the material. (After Richards et al (1984)).

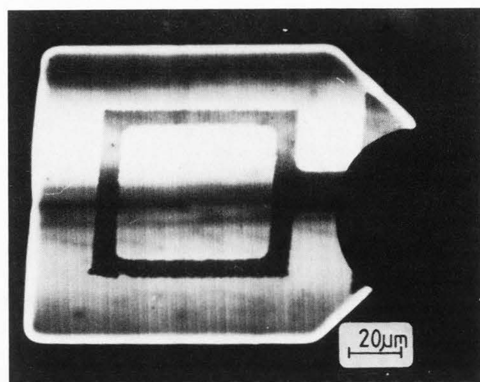

Fig. 16. Dark lines in an electroluminescent light optical microscope picture of a GaAs LED. (After Trigg and Richards (1982).

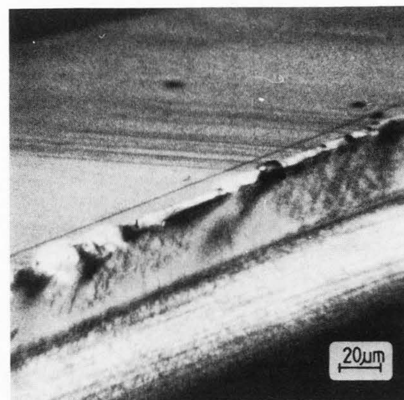

Fig. 17. The type of slip planes in the epitaxial layer that were responsible for the effect in Figure 16, seen in a panchromatic CL SEM micrograph (After Trigg and Richards (1982)).

Trigg and Richards (1982) published a study of electroluminescence dark lines in high brightness GaAs LEDs as shown in Figure 16. They showed that these dark lines were due to slip planes resolvable in CL micrographs of the starting epitaxial layers as shown in Figure 17. Thus dislocations continue to be a practical problem in III-V devices. CL microscopy located the source of the trouble in the as-grown material in this case, and not in the device processing. Dislocations are undesirable in optoelectronic materials both for the enhanced recombination that they may produce themselves, and because they produce impurity segregation into Cottrell atmospheres and precipitates.

Dislocation CL Contrast Studies

Dislocations produce dark contrast in intrinsic CL micrographs (e.g., in GaAs and GaP) but they can produce bright contrast in extrinsic micrographs at certain wavelengths (e.g., in diamonds). A serious problem in the study of the electrical and optical effects of dislocations is that of avoiding impurity segregation to the dislocation core (e.g., Holt (1979)). The first evidence of dark contrast in CL micrographs due to relatively "clean" dislocations introduced by plastic deformation was that produced by Esquivel et al (1973) in GaAs and Davidson et al (1975) in GaP. Titchmarsh et al (1977) in studies of GaP and Pennycook and Brown (1979) in studies of divalent oxides concluded that the contrast due to enhanced recombination was probably produced by the core structure of the dislocations. Consequently they concluded that information should be obtainable concerning the energy bands arising from the dislocations. A large body of work using other techniques leads to the conclusion that there are two types of localized electronic energy states associated with dislocations: deep (mid-gap) levels associated with dangling bonds and shallow states arising from the elastic strain field via the deformation potential. Overlap of the wave functions leads to the formation of a number of energy bands in the forbidden energy gap from these states. For a brief review see e.g. Holt and Lesniak (1985) and the proceedings of the most recent conference in this field: the Aussois Symposium (J. de Phys. Colloque C4 (1983)). This possibility is the reason for the fundamental interest in dislocation CL contrast studies. There is a similar interest in the EBIC contrast of dislocations for the same reason (see Holt and Lesniak (1985)).

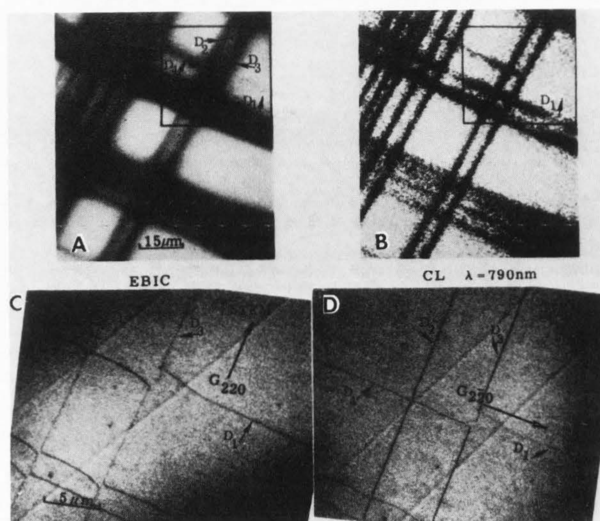

Fig. 18. (A) EBIC, (B)CL and (C)STEM micrographs of a misfit dislocation network in epitaxial $Ga_{1-x}Al_xAs_{1-y}P_y$ material. Dislocation D1 in (C) is a sessile edge which does not give EBIC and CL contrast unlike the others which are all 60° misfit dislocations (After Petroff et al (1980)).

The use of a combination of CL, Charge Collection (CC), (EBIC) and STEM (or TEM) microscopy (Petroff et al (1980) and Pennycook and Brown (1980)) is particularly powerful as Figure 18 illustrates. The observation in this

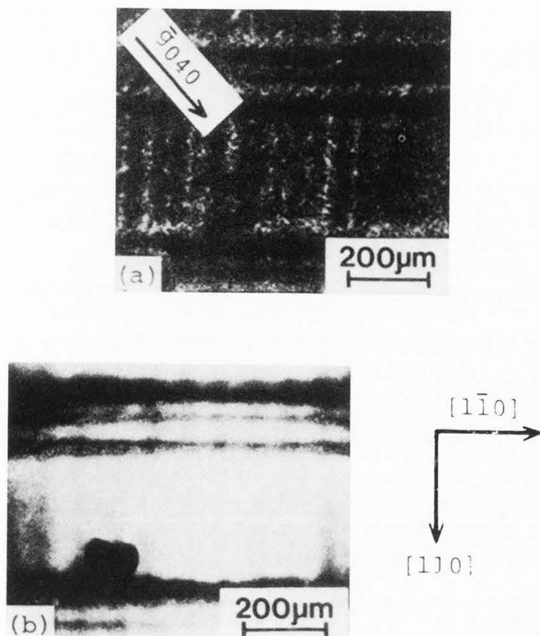

Fig. 19. Asymmetry of the PL contrast properties of the two grids of <110> misfit dislocations in an interface between InGaAsP and InP. (a) X-ray topograph showing both orthogonal grids and (b) scanning PL micrograph, with the InGaAsP excited, showing only the horizontal grid to have strong PL contrast. (After Yamaguchi et al (1981)).

case that certain types of dislocation give rise to CL and EBIC contrast, while others do not is among the strongest evidence that core effects are involved. Another example of such evidence was that of Yamaguchi et al (1981) that of the two orthogonal sets of misfit dislocations in InGaAsP/InP (100) heterojunctions, only one gives rise to strong PL contrast as Figure 19 shows. (Yamaguchi et al used a scanning "spatially resolved PL" microscopy technique.) The two sets of orthogonal misfit dislocations in heterojunctions in (100) orientation are not crystallographically equivalent and so are presumably of different polarity i.e., one set is of α - and the other of β - dislocations (see e.g. Holt (1979)). The interpretation of the observations of Yamaguchi et al is not simple. The micrograph of Figure 19(b) was recorded with the PL from the InGaAsP layer whereas X-ray topographic evidence showed the misfit dislocations to lie in the InP. Thus the difference in core structure is manifested in a difference in recombination at a distance. A core-polarity - dependent impurity atmosphere effect could thus be involved.

Dark CL dislocation contrast can be measured as a reduction in the signal level from L_B in the bulk to L_D at the defect minimum in CL line scans across dark lines. The contrast is usually defined as

$$C = (L_B - L_D)/L_B \tag{16}$$

Attempts to interpret the reduction in CL intensity or photon count rate L in terms of the effect of the dislocation run into the problem expressed by equation (10). This is that a reduction in the rate of radiative recombination, R_{rri} and an increase in the rate of non-radiative recombination R_{nri} are indistinguishable from L or η_{rri} measurements alone. Early measurements on the shift in the CL wavelength for the maximum intensity in Se-doped GaAs (Balk et al (1976)) indicated that the dislocation CL contrast arose from a Cottrell atmosphere about the defect. Steckenborn et al (1981) used a digitized CL system to measure both intensity and lifetimes at the points of a 126 x 126 grid. This was applied to an area centred on the point at which a dislocation emerged through the surface of a specimen of Se-doped GaAs. This showed that the intensity minimum, constituting the dark contrast was fairly symmetrical and about 20 µm wide. The peak in the lifetime was however only about half as wide. This shows that the segregation of a single type of recombination centre to the dislocation cannot account for the contrast in this case. (See also Queisser and Fuller (1966), Davidson and Rasul(1977), Rasul and Davidson. (1977) and Brown et al (1983)).

Dislocations in diamond exhibit bright contrast at different wavelengths in the visible range (Hanley et al (1977)). Kiflawi and Lang (1974) reported that the CL from dislocations in diamond was linearly polarized. Berger and Brown (1984) found that virtually all the visible CL from semiconducting type IIb diamonds comes from dislocations whereas none of the visible CL from type IIa diamonds came from dislocations. They also found that the dislocations in type IIb diamonds were non-uniform in CL emission intensity along their length. Their conclusion was that the bright extrinsic contrast from dislocations in some natural diamonds was probably due to a donor-acceptor pair recombination mechanism.

For studies of the dislocation CL contrast in GaP Rasul and Davidson (1977) expressed the contrast in terms of the recombination rates and hence of the bulk minority carrier lifetime τ_B and the reduced lifetime at the dislocation τ_D using equation (10). Independent measurements of the contrast and of the lifetimes in the bulk and at the dislocation, τ_B and τ_D, gave reasonable agreement. This work was reviewed previously (Holt and Datta (1980)). Similar measurements were reported by Chu et al (1981) and Hastenrath and Kubalek (1982). This recent work on GaAs still gave strong evidence of impurity segregation as a major factor in dislocation CL contrast. It is known from EBIC studies of Si that contrast of tens of percent is obtained for decorated dislocations whereas clean dislocations give contrast of a percent at most. Possibly similar results will be found when genuinely atomically clean dislocations in III-V compounds are examined in CL micrographs.

More recently Lohnert and Kubalek (1983) modified the well-known Donalato theory for the charge collection (CC or EBIC) contrast of dislocations for CL contrast. The

dislocation was treated as a cylindrical volume of radius Ro within which the minority carrier lifetime is reduced from τ to τ' with the sort of effect on the beam-induced carrier distribution shown in Figure 20(a). The variation of contrast with beam-dislocation distance was found to be as shown in Figure 20(b). The success and limitations of the Donalato theory of dislocation CC (EBIC) contrast is reviewed elsewhere (Holt and Lesniak (1985)).

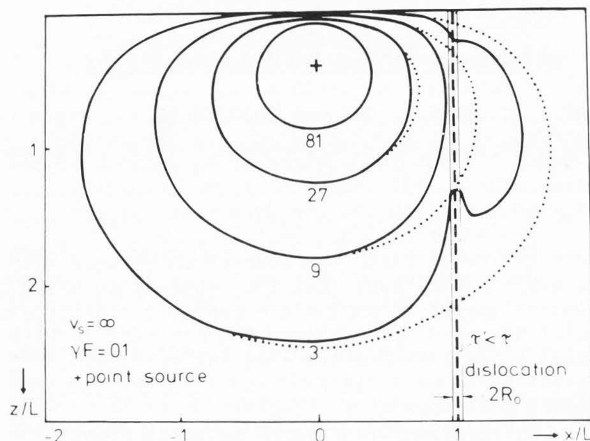

Fig. 20(a) CL dislocation contrast calculated by a modified Donalato model. (a) Isoconcentration lines of excess carrier density under the beam impact point. The dotted curves represent the case in the absence of the dislocation (vertical dashed line) and the continuous curves represent the case when the dislocation is present as shown.

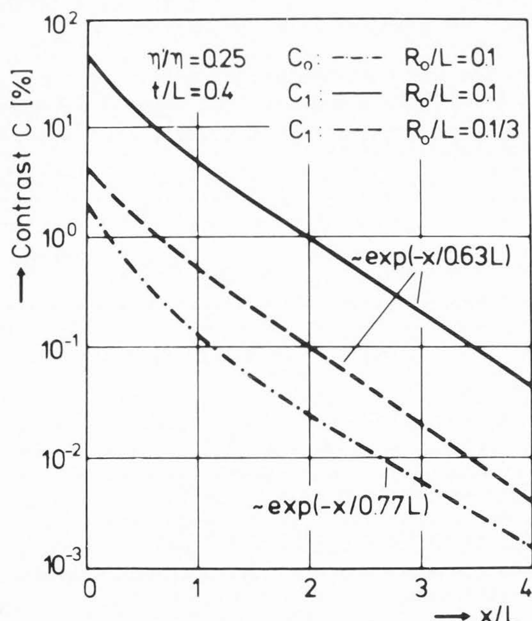

Fig. 20(b) The fall in the CL contrast with distance from the dislocation, relative to the minority carrier diffusion length for various values of the relative radius of the reduced lifetime cylinder round the dislocation (see (a)). (After Löhnert and Kubalek (1983)).

Interest in dislocation CL contrast was further increased by the availability of infra-red CL detection systems capable of microscopic observations of defects in InP (Figure 21) and in Si (Figure 22). Myhajlenko et al (1984) demonstrated that infra-red CL decay times τd can be measured using a beam-blanking, lock-in amplifier detection system. These techniques are in their infancy and there are serious experimental difficulties involved. However, the importance of Si is so great that the effort in this field is likely to increase. Studies of the CL properties of dislocations in Si especially can be related to the large amount of other information, experimental and theoretical that is available.

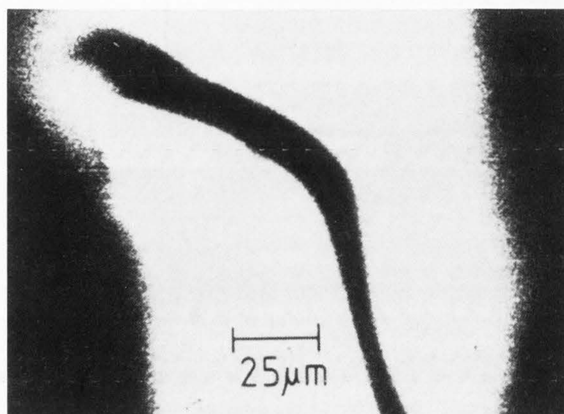

Fig. 21. Integral band edge CL micrograph of a linear defect in InP. (After Myhajlenko (1984)).

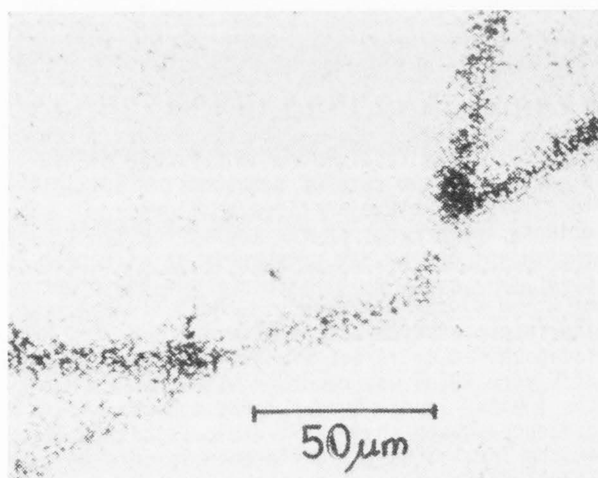

Fig. 22. Infrared CL micrograph of a grain boundary network in polycrystalline Si. (After Cumberbatch et al (1981)).

An indication of the interest in the luminescence effects of dislocation is provided by the proceedings of the International Colloquium on Properties and Structure of Dislocations in Semiconductors held at Aussois,

France in 1983.(J. de Phys. Coll. C4 (1983)). This contains seven relevant papers: a review of dislocation CL by Dupuy (1983) and papers on grain boundary CL in CdTe by Klimkiewicz and Auleytner (1983), luminescence effects of dislocations in GaP by Hamilton et al (1983), PL of dislocations in Si by Suezawa and Sumino (1983) and Ossipiyan et al (1983) and on deformation luminescence in II-VIs by Emelin et al (1983) and Bredikhin and Shmurak (1983).

Artefacts

Spurious observations are possible in the CL mode of the SEM as in any other experimental technique. The possibility of strongly luminescent contaminants, of scintillations due to back scattered electrons striking glass or polymer components of CL systems, and of incandescence from the electron gun filament reaching the detector have long been recognized and guarded against. A number of additional problems are now apparent.

Warwick and Booker (1983) reported the first SEM CL spectral artefact. This was a "ghost" peak which arose from the detection of rays that are totally internally reflected before emerging from the specimen. They demonstrated the occurrence of the effect by using aperture discs as shown in Figure 23(a) to stop such rays reaching the detector. The effect of this on the longer wavelength peak can be seen in Figures 23 (b) and (c).

S. Datta (private communication) in earlier studies of striated ZnS platelet crystals noticed that areas subjected to prolonged electron beam scanning turned dark in CL micrographs but when such crystals were re-examined after a few days the dark areas were apparently no longer there. This suggests the possibility that beam-charging of vacancies occurs. S vacancies in ZnS can capture electrons and color the material purple. Electron Spin Resonance studies (Schneider and Rauber (1967)) established that classical F-centres (Pecheur et al (1977) were formed in these (partially) ionic crystals. Such effects are known to occur in electron beam scanned areas of alkali halides (Holt et al (1968), Schulson (1971a, 1971b)). Electron beam annealing was found by Myhajlenko et al (1984) to increase the infra-red CL emission intensity of ion implanted Si as shown in Figure 24. Beam damage effects must limit the use of the CL mode in many cases as they severely do in the case of polymers (Giles (1975)) and biological specimens (Bröcker and Pfefferkorn (1979), Hörl and Roschger (1980), Holt (1984b)).

Increasing changes of intensity of CL with time of scanning were observed in III-V alloys by Wakefield. At room temperature the intensity of the whole CL spectrum can fall by a factor of 2 or 3 in a few seconds. At liquid helium temperatures the intensity of the CL spectrum can increase by twenty times and still continue to rise after an hour. Such changes will present problems in attempts at quantitative analysis.

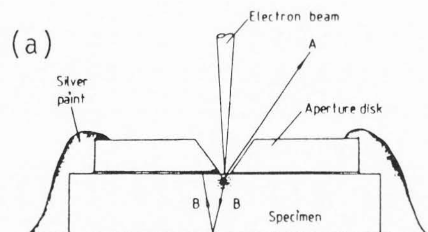

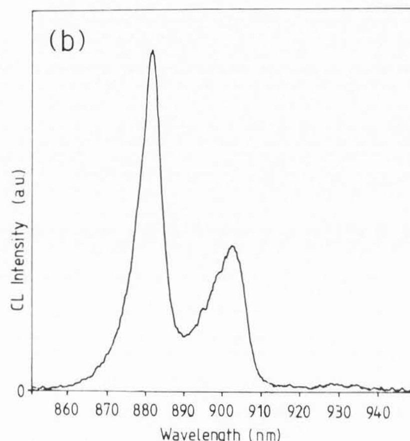

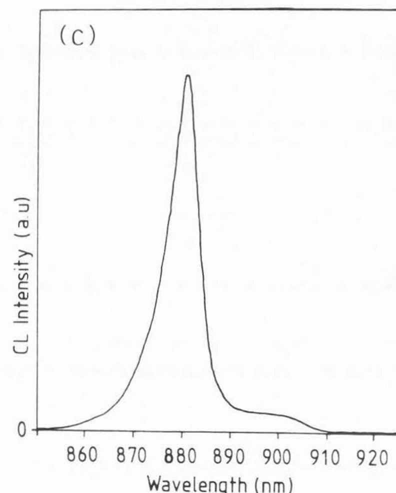

Fig. 23 (a) The origin of a "ghost" CL peak in InP slab specimens is the detection of rays following paths like B. The use of an aperture disc can stop such rays. InP spectra recorded with (b) no aperture and (c) one of 10µm diameter. The 883 nm peak is the band-band CL and the ghost peak is at 900 nm at 88 K. (After Warwick and Booker (1983)).

Artefacts must thus be guarded against in using the CL mode. It is desirable that beam induced changes in the CL emission of the materials concerned should be studied as a part of the development of the technique. A number of effects of interest in themselves are likely to be involved.

Acknowledgements

It is a pleasure to thank Dr. B.P. Richards of the Hirst Research Centre of GEC Ltd. and Dr. B. Wakefield of British Telecom Research Laboratory for helpful discussions. Discussions with the late Dr. P.J. Dean were also most valuable.

LIST OF SYMBOLS

$\delta\sigma$ resolution of an FTS.

E_A energy "depth" of an acceptor level above the valence band edge.

E_D the energy depth of a donor level below the conduction band edge.

E_g the forbidden gap energy.

$E_{x(n)}$ the binding energy of the nth quantum state of an exciton.

e the charge on an electron.

ε the dielectric constant

FFT fast Fourier transform computational method.

FTS Fourier transform spectrometer.

h Planck's constant.

L the path difference between the two arms of the interferometer of an FTS.

L(0) the intensity or photon emission rate of the (CL) light at time t = 0 when the beam was chopped.

L(t) the intensity of the light a time t later.

L_i the photon emission rate in the ith CL band.

L_B the intensity of the CL from the bulk of the material.

L_D the intensity of the CL emitted with the beam incident on a dislocation.

λ the CL wavelength.

N number of CL spectral elements recorded.

$\bar{N}$ the average number of phonons emitted with an "edge" photon.

η_{rri} radiative efficiency of the ith re-combination CL band.

ν_f the frequency of the intensity peak of the fundamental CL emission band.

r separation of donor-acceptor pairs in a crystal.

R_{rri} the rate of recombination via the ith radiative centres.

σ_M maximum wave number (reciprocal of the shortest wavelength) detected.

T total spectral measurement time.

τ_B the minority carrier lifetime in bulk (good) material.

τ_D the minority carrier lifetime at a dislocation.

τ_d CL decay time.

τ_{rri} the recombination time of the ith radiative centres.

τ_{nri} the effective total non-radiative recombination time for the ith CL radiative recombination band.

τ_{rri} recombination time of the jth radiative centres.

τ_{nri} recombination time of the jth non-radiative centres.

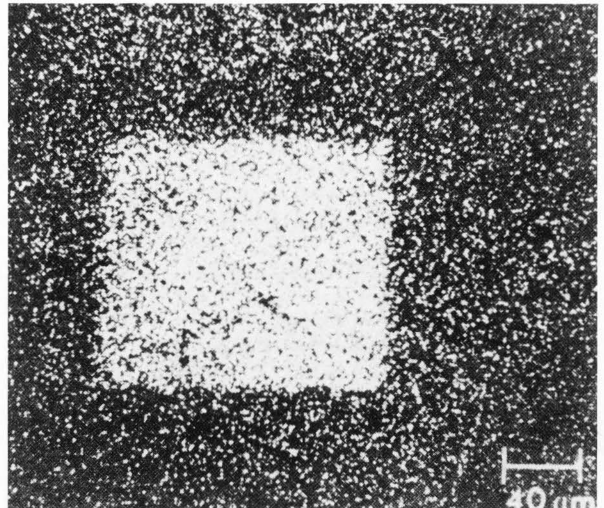

Fig. 24. An infrared CL micrograph of ion implanted Si showing a bright patch resulting from electron beam annealing (After Myhajlenko et al (1983b)).

References

Acuna Rojas CM, Holt DB, Yacobi BG. (1980) Further SEM Studies of GaP Electroluminescent Diodes. J. Mat. Sci. 15, 1276-1282.

Almassy RJ, Reynolds DC, Litton CW, Bajaj KK, McCoy GL. (1981) Observation of Shallow Residual Donors in High Purity Epitaxial Gallium Arsenide by Photoluminescence Spectroscopy. Solid State Communications 38, 1053-1056.

Ashen DJ, Dean PJ, Hurle DTJ, Mullin JB, White AM. (1975) The Incorporation and Characterization of Acceptors in Epitaxial GaAs. J. Phys. Chem. Solids 36, 1041-1053.

Balk LJ, Kubalek E, Menzel E. (1976) Investigations of As-grown Dislocations in GaAs Single Crystals in the SEM. Scanning Electron Microsc. 1976; I: 257-264.

Balk LJ, Kubalek E, Menzel E. (1975) Time-Resolved and Temperature-Dependent Measurements of Electron Beam Induced Current, Voltage, and CL in the SEM. Scanning Electron Microsc. 1975: 447-455.

Bebb HB, Williams EW. (1972) Photoluminescence I. Theory, in Semiconductors and Semimetals Vol. 8 (RK Willardson, AC Beer, Editors) Academic Press, New York pp. 181-320.

Berger SD, Brown LM. (1984) Cathodoluminescence from Dislocations in Type II Natural Diamond, in Electron Microscopy and Analysis, 1983. Conf. Series No. 68 (P. Doig, Editor) Inst. Phys., Bristol and London pp. 115-118.

Bernholc J, Lipari NO, Pantelides ST, Scheffler M. (1981) Theory of Point Defects and Deep Impurities in Semiconductors, in Defects and Radiation Effects in Semiconductors 1980. Conf. Series. No. 57 (RR Hasiguti, Editor) Inst. Phys.: Bristol and London 1981 pp. 1-17.

Blasse G. (1978) Materials Science, in the Luminescence of Inorganic Solids (B. Di Bartolo, Editor) Plenum Press, New York pp. 457-494.

Booker GR. (1981) Developments in Semiconducting Materials Applications of the SEM, in Microscopy of Semiconducting Materials, Conf. Series No. 60, AG Cullis, DC Joy (eds.), Inst. Phys. Bristol and London, 203-214.

Bredikhin SI, Shmurak SZ. (1983) Deformation Luminescence in II-VI Crystals. International Colloquium on Properties and Structure of Dislocations in Semiconductors, Aussois, France, March, 1983. Supplement to J. de Phys. Colloque C4 pp. C4-183, C4-188.

Broecker W, Pfefferkorn G. (1978) Bibliography on Cathodoluminescence. Scanning Electron Microsc. 1978; I: 333-351.

Broecker W, Pfefferkorn G. (1979) Applications of the Cathodoluminescence Method in Biology and Medicine. Scanning Electron Microsc. 1979; II: 125-132.

Broecker W, Pfefferkorn G. (1980) Bibliography on Cathodoluminescence Part II. Scanning Electron Microsc. 1980; I: 298-302.

Brown GT, Warwick CA, Young IM, Booker GR. (1983) An Examination of Dislocations in Si-doped LEC GaAs by Double Crystal X-ray Topography, SEM Cathodoluminescence and Chemical Etching, in Microscopy of Semiconducting Materials, Conf. Series No. 67 AG Cullis, SM Davidson, GR Booker (eds.), Inst. Phys., Bristol and London, 371-376.

Chin AK. (1982) A Simple, High Collection Efficiency Cathodoluminescence Imaging Technique: Application to GaSb and CdTe. Scanning Electron Microsc. 1982; III: 1069-1075.

Chin AK, Temkin H. Roedel RJ. (1979) Transmission Cathodoluminescence: A New SEM Technique to Study Defects in Bulk Semiconductor Samples. Appl. Phys. Lett. 34, 476-477.

Chin AK, Temkin H. Mahajan S, Bonner WA, Ballman AA and Dentai AG. (1976) Evaluation of Defects in InP and In GaAsP by Transmission Cathodoluminescence. J. Appl. Phys. 50, 5707-5709.

Chu YM, Darby DB, Booker GR. (1981) SEM CL and TEM Studies of Te- and Si-doped GaAs, in Microscopy of Semiconducting Materials, ibid., 331-338.

Clark S, Stirland DJ. (1981) Dislocation Density Variations Across Semi-insulating GaAs Substrates, in Microscopy of Semiconducting Materials, ibid., 339-344.

Cocito M, Papuzza C, Taiariol F. (1983) Emission and Transmission Cathodoluminescence Analysis of InGaAsP/InP LPE Double Heterostructures Emitting at 1.3 and 1.6, in: Microscopy of Semiconducting Materials, Conf. Series No. 67 AG Cullis, SM Davidson, GR Booker (eds.), Inst. Phys., Bristol & London, 273-278.

Cooley JW and Tukey JW (1965) An Algorithm for Machine Calculation of Complex Fourier Series Maths Comput. 19, 297-301.

Cumberbatch TJ, Davidson SM, Myhajlenko S. (1981) Cathodoluminescence Imaging of Silicon, in Microscopy of Semiconducting Materials, ibid., 197-202.

Datta S, Yacobi BG, Holt DB. (1977) Scanning Electron Microscope Studies of Local Variations in Cathodoluminescence in Striated ZnS Platelets. J. Mat. Sci. 12, 2411-2420.

Davidson SM, (1977) Semiconductor Material Assessment by Scanning Electron Microscopy. J. Microscopy 110, 177-204.

Davidson SM, Dimitriadis, CA (1980) Advances in the Electrical Assessment of Semiconductors Using the Scanning Electron Microscope. J. Microscopy 118, 275-290.

Davidson SM, Rasul A. (1977) Applications of a High Performance SEM-based CL Analysis System to Compound Semiconductor Devices. Scanning Electron Microsc. 1977; I: 225-232.

Davidson SM, Cumberbatch TJ, Huang E, Myhajlenko S. (1981) A New Scanning Cathodoluminescence Microprobe System, in Microscopy of Semiconducting Materials, ibid., 191-196.

Davidson SM, Iqbal MZ, Northrop DC. (1975) SEM Cathodoluminescence Studies of Dislocation Recombination in GaP. Phys. Stat. Sol. a29, 571-578.

Dean PJ. (1982) Photoluminescence as a Diagnostic for Semiconductors. Cryst. Growth Characteriz. 5, 89-174.

Di Bartolo B. (1978) Interaction of Radiation with Ions in Solids, in Luminescence of Inorganic Solids (B. Di Bartolo, Editor) Plenum Press, New York,

Duncan KR, Eaves L, Ramdane A, Roys WB, Skolnick MS, Dean PJ. (1984) An Investigation of the 1.36eV Photoluminescence Spectrum of Heat-Treated InP Using Zeeman Spectroscopy and Strain Effects. J. Phys. (C) Sol. State Phys. 17, 1233-1245.

Dupuy M. (1983) Cathodoluminescence Studies of Dislocations in Semiconductors. J. de Phys. Colloque C-4, ibid., pp. C4-277 to C4-287.

Emelin V Ya, Klassen NV, Negrii VD, and Ossipiyan Yu A. (1983) Optical Properties of Plastically Deformed AII BVI Crystals. J. de Phys. Colloque C-4, ibid., pp. C4-125 to C4-132.

Esquivel AL, Lin WN, Wittry DB. (1973) Cathodoluminescence Study of Plastically Deformed GaAs. Appl. Phys. Lett. 22, 414-416.

Giles PL. (1975) Cathodoluminescence. J. de Microscopie 22, 357-370.

Haefner H, Morawetz H, Oelgart G. (1981) Cathodoluminescence Measurements on Green Light-Emitting GaP Diodes. Phys. Sol. a63, 495-500.

Hamilton B, Peaker AR, Wight DR. (1983) Luminescence and Deep Level Studies of Line Dislocations in Gallium Phosphide. J. de Phys. Colloque C-4, ibid., pp. C4-233 to C4-241.

Hanley PL, Kiflawi I, Lang AR. (1977) On Topographically Identifiable Sources of Cathodoluminescence in Natural Diamonds. Phil. Trans. Roy. Soc. A284, 329-368.

Hastenrath M, Balk LJ, Lohnert K, Kubalek E. (1977) Time Resolved Cathodoluminescence in the Scanning Electron Microscope by Use of the Streak Technique. J. Microscopy 118, 303-308.

Hastenrath M, Kubalek E. (1982) Time-Resolved Cathodoluminescence in Scanning Electron Microscopy. Scanning Electron Microsc. 1982; I: 157-173.

Holt DB. (1974) Quantitative SEM Studies of CL in Adamantine Semiconductors, in Quantitative Scanning Electron Microscopy (DB Holt, MD Muir, PR Grant, IM Boswarva, Editors) Academic Press, London pp. 335-386.

Holt DB. (1979) Device Effects of Dislocations. International Symposium on Dislocations in Tetrahedrally Coordinated Semiconductors, Hunfeld/Fulda (FRG), September, 1978. Supplement to J. de Physique Colloque C6, pp. C6-189 to C6-199.

Holt DB. (1981) Recent Developments in SEM Detection Systems for the Cathodoluminescence and Conductive Modes, in Microscopy of Semiconducting Materials, ibid., 165-178.

Holt DB. (1984) Cathodoluminescence Mode Scanning Electron Microscopy in The Analysis of Organic and Biological Surfaces (P. Echlin, Editor) (Wiley, New York) pp. 301-324.

Holt DB, (1985) Microcharacterization of Crystals Using the Scanning Electron Microscope in Crystal Growth of Electronic Materials. (E. Kaldis, Editor) (Elsevier Science) pp. 343-358.

Holt DB, Datta S. (1980) The Cathodoluminescent Mode as an Analytical Technique: Its Development and Prospects. Scanning Electron Microsc. 1980; I: 259-278.

Holt DB, Lesniak M. (1985) Recent Developments in Electrical Microcharacterization Using the CC Mode of the SEM. Scanning Electron Microsc. 1985; I: 67-86.

Holt DB, Gavrilovic J, Jones MP. (1968) Scanning-Electron Beam Anomalous Transmission Patterns. J. Mat. Sci. 3, 553-558.

Hopfield JJ. (1959) A Theory of Edge-Emission Phenomena in CdS, ZnS and ZnO. J. Phys. Chem Solids 10, 110-119.

Hörl, EM, Roschger P. (1980) CL SEM Investigations of Biological Material at Liquid Helium and Liquid Nitrogen Temperatures. Scanning Electron Microsc. 1980; I: 285-292.

Horlick G. (1968) Introduction to Fourier Transform Spectroscopy. Appl. Spectrosc. 22, 617-626.

Kamejima T, Shimura F, Matsumoto Y, Watanabe H and Matsui J. (1982) Role of Dislocations in Semi-Insulation Mechanism in Undoped LEC GaAs Crystal. Japan. J. Appl. Phys. 21, L721-L723.

Kiflawi I, Lang AR. (1974) Linearly Polarized Luminescence from Linear Defects in Natural and Synthetic Diamond. Phil. Mag. 30, 219-223.

Klimkiewicz M, Auleytner J. (1983) X-ray and Scanning Cathodoluminescence Imaging of Small-angle Grain Boundaries and Dislocations in CdTe Crystals. J. de Phys. Colloque C-4, ibid., pp. C4-313 to C4-316.

Lee TC, Anderson WW. (1964) Edge Emission Involving Manganese Impurities in GaAs at 4.2K. Sol. State Commun. 2, 265-268.

Löhnert K, Kubalek E. (1983) Characterization of Semiconducting Materials and Devices by EBIC and CL Techniques, in Microscopy of Semiconducting Materials, ibid., 303-314.

Mott NF. (1978) Recombination: A Survey. Sol. State Electron 21, 1275-1280.

Myhajlenko S. (1984) Near Infrared Cathodoluminescence Assessment of Semiconductors in a TEM, in Electron Microscopy and Analysis, 1983 Conf. Series No. 68 (P. Doig, Editor) Inst. Phys., Bristol and London, pp. 111-114.

Oelgart G, Haefner H, Reulke R, Joachim F. (1982) Degradation of Green Light-Emitting GaP: N Diodes. Phys. Stat. Sol. a71, 89-98.

Ossipiyan Yu.A, Rtishchev AM, Steinman EA. (1983) The Effect of Hydrogen on Dislocation Photoluminescence in Silicon. J. de Phys. Colloque C-4, ibid., pp. C4-255 to C4-259.

Pecheur P, Kauffer E, Gerl M. (1977) A Tight-binding Model of the ZnS F-centre, in Radiation Effects in Semiconductors 1976. Conf. Series No. 31 Inst. Phys., Bristol and London pp. 458-464.

Pennycook SJ, Brown LM. (1979) Cathodoluminescence at Dislocations in Divalent Oxides. J. Luminescence 18/19, 905-909.

Pennycook SJ, Brown LM, Craven AJ. (1980) Observation of Cathodoluminescence at Single Dislocations by STEM. Phil. Mag. A41, 589-600.

Petroff PM, Logan RA, Savage A. (1980) Nonradiative Recombination at Dislocations in III-V Compound Semiconductors. Phys. Rev. Letters 44, 287-291.

Pfefferkorn G, Bröcker W, Hastenrath M. (1980) The Cathodoluminescent Method in the Scanning Electron Microscope. Scanning Electron Microsc. 1980; I: 250-258.

Queisser HJ, Fuller CS. (1966) Photoluminescence of Cu-Doped Gallium Arsenide. J. Appl. Phys. 37, 4895-4899.

Rasul A, Davidson SM. (1977) SEM Measurements of Minority Carrier Lifetimes at Dislocations in GaP, Employing Photon Counting. Scanning Electron Microsc. 1977; I: 233-240.

Richards BP, Trigg AD, King WG. (1984) Investigation of Fluorescent Lamp Phosphors Using the Combined CL and EDS Modes of the SEM. Scanning 6, 8-19.

Saba FM, Holt DB. (1983) A Low-Temperature, High-Resolution, Computer Controlled SEM CL Detection System, in Microscopy of Semiconducting Materials, ibid., 333-336.

Sakai H. (1977) High Resolving Power Fourier Spectroscopy in Spectrometric Techniques Vol. 1 (G.A. Vanasse, Editor) (Academic Press: New York) pp. 1-70.

Schiller C, Bois D. (1974) Observation des Defauts dans les Semiconducteurs par Microscopie a Balayage en Cathodoluminescence. Rev. de Physique Appl. 9, 361-371.

Schneider J, Rauber A. (1967) Electron Spin Resonance of the F-centre in ZnS. Sol. State Commun. 5, 779-781.

Schopper HW and Thompson RJ. (1974) Fourier Spectrometers, in Methods of Experimental Physics. Vol. 12. Astrophysics, Part A: Optical and Infrared (N Carlton, Editor) (Academic Press: New York).

Schulson EM. (1971a) SEM Electron Channelling Line Width (Broadening) and Pattern Degradation in Alkali Halide Crystals. Scanning Electron Microsc. 1971: 489-496.

Schulson EM. (1971b) A Scanning Electron Microscope Study of the Degradation of Electron Channelling Effects in Alkali Halide Crystals during Electron Irradiation. J. Mat. Sci. 6, 377-383.

Spivak GV, Saparin GV, Komolova LF. (1977) The Physical Fundamentals of the Resolution Enhancement in the SEM for CL and EBIC-Modes. Scanning Electron Microsc. 1977; I: 191-200.

Steckenborn A, Münzel H, Bimberg D. (1981) Cathodoluminescence Lifetime Pattern of Semiconductor Surfaces and Structures, in: Microscopy of Semiconducting Materials, Conf. Ser. no. 60, AG Cullis, DC Joy (eds.), Inst. Phys. Bristol and London, 185-190.

Stegmann R, Kloth B, Oelgart G. (1982) The Temperature Dependence of Luminescence Intensity in $GaAs_{1-x}P_x$:N. Phys. Stat. Sol. a70, 423-431.

Steyn JB, Giles PL, Holt DB. (1976) An Efficient Detection System for Cathodoluminescence Mode Scanning Electron Microscopy. J. Microscopy 107, 107-128.

Stirland DJ, Grant I, Brozel MR, Ware RM. (1983) Microscopic Examination of the Deep Donor EL2 in Undoped Semi-insulating GaAs, in Microscopy of Semiconducting Materials, ibid., 285-290.

Suezawa M, Sumino K. (1983) Photoluminescence from Dislocated Silicon Crystals. J. de Phys. Colloque C-4, ibid., pp. C4-133 to C4-139.

Temkin H, Dutt BV, Bonner WA and Keramides VG. (1982) Deep Radiative Levels in InP. J. Appl. Phys. 53, 7526-7533.

Titchmarsh JM, Booker GR, Harding W, Wight DR. (1977) Carrier Recombination at Dislocations in Epitaxial Gallium Phosphide Layers. J. Mat. Sci. 12, 341-346.

Trigg AD, Richards BP. (1982) Correlation of LED Device Performance with Materials and Processing Using CL and EBIC Techniques. IEE Proc. 129, 33-38.

Wakefield B. (1983) Low Temperature Cathodoluminescence of Life-Tested GaAsAs/GaAs Double Heterostructure Lasers, in Microscopy of Semiconducting Materials, ibid., 315-320.

Wakefield B, Eaves L, Prior KA, Nelson AW, Davies GJ. (1984a) The 1.36 eV Radiative Transition in InP: Its Dependence on Growth Conditions in MBE and MOCVD Material. J. Phys. D Appl. Phys. 17, L133-L136.

Wakefield B, Leigh PA, Lyons MH, Elliott CR. (1984b) Characterization of Semi-insulating Liquid Encapsulated Czochralski GaAs by Cathodoluminescence. Appl. Phys. Lett. 45, 66-68.

Warwick CA, Booker GR. (1983) Use of SEM CL Spectra to Determine Local Variations in Ge Doping Concentration in LEC InP Ingots, in Microscopy of Semiconducting Materials, ibid., 321-326.

Werkhoven C, van Opdorp C, Vink AT. (1978/79) Influence of Crystal Defects on the Luminescence of GaP. Philips Tech. Rev. 38, 41-50.

Williams EW, Bebb HB. (1972) Photoluminescence II: Gallium Arsenide, in Semiconductors and Semimetals Vol. 8 (RK Willardson, AC Beer, Editors) Academic Press, New York pp. 321-392.

Williams EW, Elder W, Astles MG, Webb M, Mullin JB, Straughan B, Tufton PJ. (1973) Indium Phosphide I. A Photoluminescence Materials Study. J. Electrochem. Soc. 120, 1741-1749.

Yacobi BG, Datta S, Holt DB. (1978) The Form of the Edge Emission Band in CdS and ZnS Crystals. Phil. Mag. 35, 145-158.

Yacobi BG, Datta S, Holt DB. (1979) The Shape of the Self-Activated Cathodoluminescence Band in ZnS:Cl Crystals. J. Luminescence. 21, 53-73.

Yamaguchi A, Komiya S, Ueda O, Nakajima K, Umebu I, Akita K. (1981) Asymmetric Character of Misfit Dislocations in LPE DH InGaAsP/InP, in Gallium Arsenide and Related Compounds 1981. Conf Series No. 63. (T Sugano, Editor) Inst. Phys., Bristol and London pp. 161-166.

Yu PW, Park YS. (1979) Photoluminescence in Mn-implanted GaAs - An Explanation of the 1.40 eV Emission. J. Appl. Phys. 50, 1097-1103.

Discussion with Reviewers

L.J. Balk: How do you think is the chance to detect CL signal at real infrared, for instance by use of PbTe-detectors or TGS/DTGS cameras (in OMA Systems)?
Authors: We suspect that it is premature to attempt so ambitious an instrumental development. Little or nothing is yet known about the intensities of infrared signal that can be obtained in a SEM, and infrared detectors are undergoing rapid development. We would prefer to comment later, when we and others have more experience in the near infrared and when GaInAsP PIN, APD, and CdHgTe detector technologies have matured.

L.J. Balk: How do you judge on the possibility of determining the behaviour of deep traps by CL?
Authors: Some information on deep traps such as Mn in GaAs has already been obtained via the SEM as mentioned above, and other results of this type will no doubt appear. Clearly only luminescent centres can be detected and, concerning these, the PL method is likely to continue to provide more spectroscopic information due to the larger intensities obtainable by exciting bulk samples. This means that higher spectral resolutions can be obtained than for SEM CL. Moreover, since the specimens for PL are not on a stage inside a specimen chamber, they can be subjected to a wide range of influences such as electric and magnetic fields and elastic stresses. This makes "modulation spectroscopy" possible and helps greatly to identify the symmetry of the site occupied by the centre, etc. An advantage of SEM CL is its spatial resolution with the ability that confers to observe local differences in the centres occurring due to diffusion, segregation, complex formation, etc. (See, for example, the work on Cu in CdTe by J.P. Chamonel, E. Molva, M. Dupuy, R. Accomo and J.L. Pautrat (1983). Spectral Resolution in Low Temperature Cathodoluminescence. Application to CdTe. Physica 116B, 519-526.) It is also possible that SEM CL observations in many particular future cases may precede and inspire detailed low temperature PL analyses. A second advantage is that SEM CL data can be compared with X-ray, CC and, perhaps, scanning Auger or scanning deep level trap spectroscopic data also obtained in the SEM.

L.J. Balk: Can you comment on the possibility of producing stimulated (coherent) CL emission?
Authors: There was a considerable body of work done on cathodoluminescent laser action in II-VI compounds in the 1960s. It was successfully observed, using flood beam excitation, in all the Cd and Zn chalcogenides as well as ZnO and Cd(S:Se) alloys. For references and some discuscussion of possible effects in the SEM see Holt (1974) pp. 371-374. We do not know of any subsequent work in this field.

L.J. Balk: The discussion on "arbitrary units" versus absolute CL numbers seems to claim that by these absolute values a quantitative measure of a material parameter can be gained. This might not be true in any case, as the interior CL yield might be affected by varying surface properties in such a manner that the external, i.e. the detectable, signal is falsified.
Authors: This is quite correct and attempts to calculate the more physically significant internally generated spectrum from the externally observed emission spectrum have hardly begun. Both to simplify the calculation and to avoid the sort of variable surface effects you allude to, it will be desirable to develop standardized surface treatments as well as specimen shapes such as hemispherical specimens with the planar surface scanned or effectively semi-infinite specimens with absorbing treatments on the surfaces other than on top, etc.

M. Cocito: Can you briefly discuss the relative merits of Spatially Resolved Photoluminescence and Spectral Cathodoluminescence?
Authors: Spatially resolved PL and SEM CL are comparable techniques. To obtain spatial resolution comparable to that available with SEM CL, PL intensities and spectral resolutions would compensatingly fall to SEM CL levels. An advantage of PL is the absence of electron beam damage, although, in attempts to obtain more intense PL, laser beam damage might be encountered. A second advantage is that there is no possibility of spectral differences arising through differences in excitation mechanisms when making comparison with high resolution PL spectra. The inconvenience of current methods for scanning light beams is considerable, and there is at present only one other mode of scanning light microscopy with which to compare the results of spatially resolved PL: OBIC(optical beam induced current).

M. Cocito: Could you comment on the commercial availability and the feasibility of routine use of FTS?
Authors: At present no Fourier transform spectrometer suitable for SEM work is commercially

available. At least one manufacturer is considering producing one, however. The increase of interest as the field develops is likely to lead to such a product appearing.

M. Cocito: Have you applied the Spectral Cathodoluminescence technique to the multilayer epitaxial structures with different energy gap materials used for optoelectronic devices?
Authors: Much of our effort in recent years has gone into instrumentation development but some results on such materials were reported by Giles et al (1976) and Holt (1981).

A.K. Chin: In reading this paper there is the impression that there is a real difference between PL and CL analysis. Please state the possible differences in PL and CL spectral measurements besides the obvious differences in excitation volume and spatial resolution.
Authors: In addition to the differences in excitation volume (which will vary with the wavelength and, hence, the absorption coefficient of the exciting radiation in the case of PL) and the spatial resolution, PL can provide a more precisely tunable excitation. That is, by varying the photon energy of the exciting radiation, this can be made just less than and then just greater than the value required to produce CL by a particular mechanism. Thus, this mechanism can be picked out in the excitation spectrum as well as in the emission spectrum. CL excitation does not allow such selective excitation of particular mechanisms except by varying the beam voltage. Using tunable dye laser excitation lines for PL gives greater excitation-energetics resolution.

Additional Reference

Giles PL, Steyn JB, Holt DB. (1976) An Efficient Detection System for Cathodoluminescence Mode Scanning Electron Microscopy. J. Microscopy 117, 117-128.